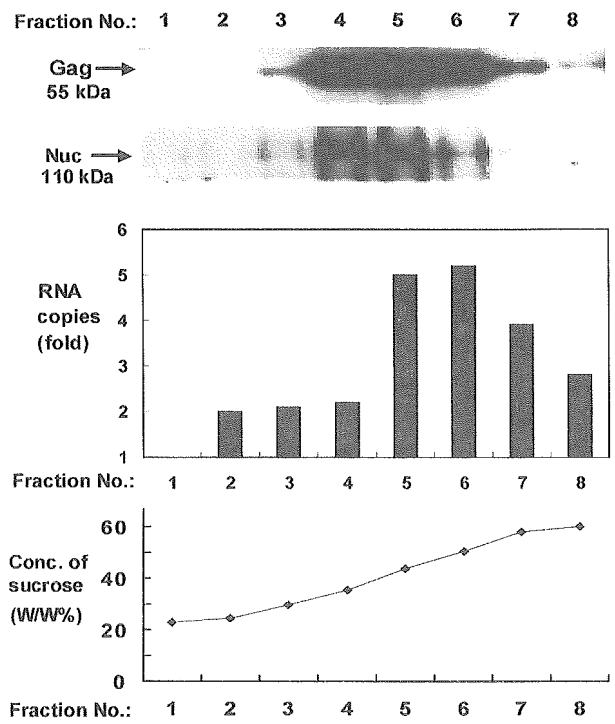


Fig. 5. Analysis of $Pr55^{gag}$, human nucleolin, and HIV-1 genomic RNA of fractionated supernatants from RK13 cells by sucrose density gradient. The supernatant from RK13 cells expressing human nucleolin and the truncated HIV-1 provirus with ψ (Fig. 1) followed by infection with rVV-$Pr55^{gag}$ was separated by sucrose density gradient, and each fraction was analyzed by a real-time RT-PCR and immunoblotting with anti-nucleolin and anti-$Pr55^{gag}$ antibodies. Black arrows indicate the positions of $Pr55^{gag}$ (Gag) and nucleolin (Nuc). The relative amounts of genomic RNA are represented as the ratio of each amount to that of fraction 1, and are shown in the form of the bar graph. The concentrations of sucrose [conc. of sucrose (w/w %)] are represented in the line graph.

5, and 6 (Fig. 6). In the presence of ψ, the ratio of the signal intensity of nucleolin to Gag proteins was 5.4 times more than that in the absence of ψ (Fig. 6). These results demonstrate that human nucleolin was incorporated into VLPs with HIV-1 genomic RNA, and that the efficiency of the incorporation was enhanced in the presence of ψ.

*The Binding of Human Nucleolin and Gag Proeins*

To analyze whether human nucleolin can bind HIV-1 gag proteins in a manner similar to that previously reported about mouse nucleolin and MuLV gag proteins (5), a human nucleolin-expressing vector was transfected into RK13 cells, following by infection of rVV-$Pr55^{gag}$. Immunoprecipitaiton analysis of the cell lysates demonstrated that gag proteins and nucleolin were co-immunoprecipitated (Fig. 7, A and B), suggesting that human nucleolin binds to HIV-1 gag proteins *in vivo*.

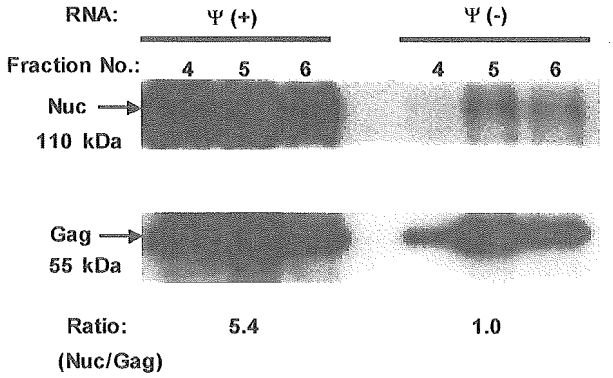


Fig. 6. Incorporation of nucleolin into VLPs with or without ψ. The supernatant from RK13 cells expressing human nucleolin and the truncated HIV-1 provirus with ψ [ψ (+)] (Fig. 1) or without ψ [ψ (−)] followed by infection with rVV-$Pr55^{gag}$ was separated by sucrose density gradient, and each fraction was analyzed by immunoblotting with anti-nucleolin and anti-gag antibodies. The results of fractions 4, 5, and 6 are shown. Black arrows indicate the positions of $Pr55^{gag}$ (Gag) and nucleolin (Nuc). The ratios of signal intensity of nucleolin to gag proteins (Nuc/Gag) in fraction 5 are indicated below the immunoblot.

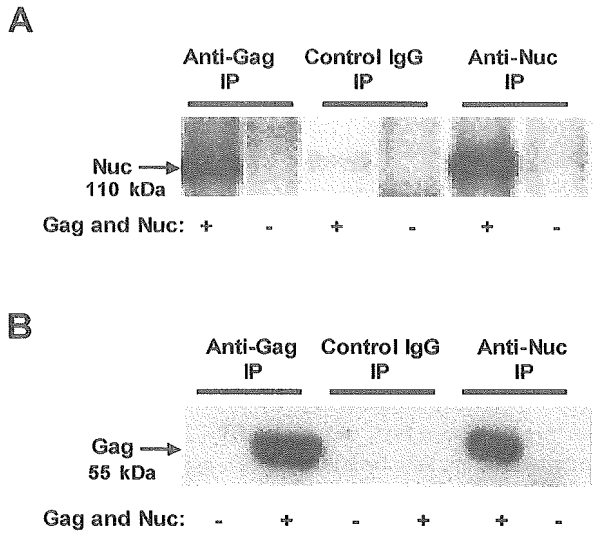


Fig. 7. Co-immunoprecipitaiton of gag proteins and nucleolin in RK13 cells. Cellular lysates from RK13 cells transfected with pch-Nuc expressing human nucleolin and infected with rVV$pr55^{gag}$ (Gag and Nuc+) or neither transfected nor infected (Gag and Nuc−), were immunoprecipitated (IP) with anti-gag (Anti-Gag), anti-nucleolin (Anti-Nuc) antibodies or control immunoglobulin G (IgG), and precipitated samples were immunoblotted with anti-nucleolin (A) and anti-gag (B) antibodies. Black arrows indicate the positions of $pr55^{gag}$ (Gag) and nucleolin (Nuc).

*Enhancement of HIV-1 Infectivity by Human Nucleolin*

Finally, we examined whether nucleolin enhances the infectivity of HIV-1. A luciferase reporter HIV-1-producing vector, pNL-Luc-E+R+, in which the *nef* gene was replaced by the luciferase gene and a human nucle-

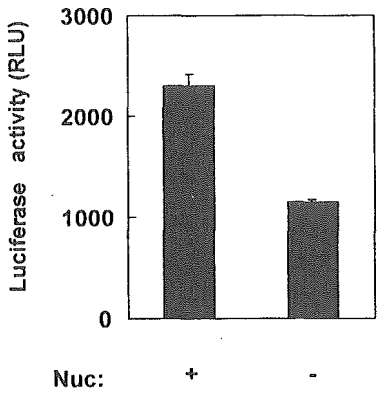


Fig. 8. The effect of nucleolin against HIV-1 infectivity. Supernatants from RK13 cells transfected with pNL-Luc-E+R+ in which the *nef* gene was replaced with the firefly luciferase gene, and pchNuc expressing human nucleolin (Nuc+) or an empty vector (Nuc−) were normalized as the p24 antigen amount and inoculated to MAGIC5 cells and luciferase activities were measured as a relative luciferase activity unit (RLU).

olin-expressing vector (Nuc+) or an empty vector (Nuc−) was introduced into RK13 cells and the supernatant was normalized as the p24 antigen amount. The total infectivity represented by the luciferase activity of HIV-1 derived from cells expressing human nucleolin increased to about twice that from cells without nucleolin expression (Fig. 8), suggesting that human nucleolin enhanced the HIV-1 infectivity.

## Discussion

In order to examine the relationships of the gag proteins, nucleolin and ψ to the infectivity of HIV-1, we initially analyzed the budding of gag proteins expressed by a recombinant vaccinia virus or HIV-1 provirus, and found that nucleolin and ψ synergistically enhanced the release of gag proteins. In addition, nucleolin and HIV-1 genomic RNA were incorporated into VLPs, and ψ enhanced the incorporation of nucleolin into VLPs.

The regulation of budding is considered to consist of the assembly of gag proteins at the plasma membrane and the release of virions (15). Recently, the assembly of gag proteins has been reported to be regulated by a cellular factor known as Tsg101, which belongs to the family of ubiquitin-conjugating enzymes (E2) and functions in vacuolar protein sorting. Tsg101 binds with HIV-1 $Pr55^{gag}$ and plays an important role in the assembly and budding of HIV-1 (8, 24). It has also been reported that HP68, a cellular ATP-binding protein, forms a complex with gag proteins and plays a critical role in HIV-1 assembly (26). Nucleolin regulates the construction of ribosomes, functions as a transporter protein between the nucleus and cytoplasm along the actin, and enhances the assembly of rRNA and ribosomal subunit proteins by binding at RNA binding domains and protein-binding domains, respectively (18, 19, 21). Although it is still unknown whether nucleolin interacts with Tsg101 or HP68, we supposed that nucleolin binds to gag proteins and ψ of HIV-1, and might be involved in the transfer of gag proteins from the nucleus to the cellular membrane. This idea was supported by several reports which stated that deleted nucleolin suppressed the budding of MuLV, HIV-1 nucleocapsid proteins bound with actin (11), and that murine nucleolin was incorporated to virions and colocalized with MuLV gag proteins (5).

The formation of nucleolin-gag protein complexes (Fig. 7) and incorporation of nucleolin (Figs. 5 and 6) into VLPs suggested that a nucleolin-gag protein complex seemed to be required for the release of virions. It has been reported that both gag proteins and nucleolin bind to a stem-loop structure in ψ (3, 10, 13, 19). Taken together, nucleolin, gag proteins and ψ might be necessary for the budding of HIV-1, and they might be incorporated into virions together. This mechanism might function to avoid the release of virions without carrying genomic RNA and to reduce the spreading of virions that cannot replicate but do enhance antigen presentation to the immune system.

In conclusion, our results provide evidence that the budding of HIV-1 gag proteins is regulated by nucleolin and ψ.

## References

1) Accola, M.A., Strack, B., and Gottlinger, H.G. 2000. Efficient particle production by minimal Gag constructs which retain the carboxy-terminal domain of human immunodeficiency virus type 1 capsid-p2 and a late assembly domain. J. Virol. **74**: 5395–5402.
2) Adachi, A., Gendelman, H.E., Koenig, S., Folks, T., Willey, R., Rabson, A., and Martin, M.A. 1986. Production of acquired immunodeficiency syndrome-associated retrovirus in human and nonhuman cells transfected with an infectious molecular clone. J. Virol. **59**: 284–291.
3) Allain, F.H., Gilbert, D.E., Bouvet, P., and Feigon, J. 2000. Solution structure of the two N-terminal RNA-binding domains of nucleolin and NMR study of the interaction with its RNA target. J. Mol. Biol. **303**: 227–241.
4) Amarasinghe, G.K., Zhou, J., Miskimon, M., Chancellor, K.J., McDonald, J.A., Matthews, A.G., Miller, R.R., Rouse, M.D., and Summers, M.F. 2001. Stem-loop SL4 of the HIV-1 psi RNA packaging signal exhibits weak affinity for the nucleocapsid protein. Structural studies and implications for genome recognition. J. Mol. Biol. **314**: 961–970.
5) Bacharach, E., Gonsky, J., Alin, K., Orlova, M., and Goff, S.P. 2000. The carboxy-terminal fragment of nucleolin interacts with the nucleocapsid domain of retroviral gag proteins and inhibits virion assembly. J. Virol. **74**: 11027–11039.

6) Bieniasz, P.D., Grdina, T.A., Bogerd, H.P., and Cullen, B.R. 1998. Recruitment of a protein complex containing Tat and cyclin T1 to TAR governs the species specificity of HIV-1 Tat. EMBO J. **17**: 7056–7065.
7) Connor, R.I., Chen, B.K., Choe, S., and Landau, N.R. 1995. Vpr is required for efficient replication of human immunodeficiency virus type-1 in mononuclear phagocytes. Virology **206**: 935–944.
8) Garrus, J.E., von Schwedler, U.K., Pornillos, O.W., Morham, S.G., Zavitz, K.H., Wang, H.E., Wettstein, D.A., Stray, K.M., Cote, M., Rich, R.L., Myszka, D.G., and Sundquist, W.I. 2001. Tsg101 and the vacuolar protein sorting pathway are essential for hiv-1 budding. Cell **107**: 55–65.
9) Hoshikawa, N., Kojima, A., Yasuda, A., Takayashiki, E., Masuko, S., Chiba, J., Sata, T., and Kurata, T. 1991. Role of the gag and pol genes of human immunodeficiency virus in the morphogenesis and maturation of retrovirus-like particles expressed by recombinant vaccinia virus: an ultrastructural study. J. Gen. Virol. **72**: 2509–2517.
10) Khan, R. and Giedroc, D.P. 1992. Recombinant human immunodeficiency virus type 1 nucleocapsid (NCp7) protein unwinds tRNA. J. Biol. Chem. **267**: 6689–6695.
11) Liu, B., Dai, R., Tian, C.J., Dawson, L., Gorelick, R., and Yu, X.F. 1999. Interaction of the human immunodeficiency virus type 1 nucleocapsid with actin. J. Virol. **73**: 2901–2908.
12) McBride, M.S. and Panganiban, A.T. 1996. The human immunodeficiency virus type 1 encapsidation site is a multipartite RNA element composed of functional hairpin structures. J. Virol. **70**: 2963–2973.
13) Meric, C. and Goff, S.P. 1989. Characterization of Moloney murine leukemia virus mutants with single-amino-acid substitutions in the Cys-His box of the nucleocapsid protein. J. Virol. **63**: 1558–1568.
14) Mochizuki, N., Otsuka, N., Matsuo, K., Shiino, T., Kojima, A., Kurata, T., Sakai, K., Yamamoto, N., Isomura, S., Dhole, T.N., Takebe, Y., Matsuda, M., and Tatsumi, M. 1999. An infectious DNA clone of HIV type 1 subtype C. AIDS Res. Hum. Retroviruses **15**: 1321–1324.
15) Nisole, S., Krust, B., Callebaut, C., Guichard, G., Muller, S., Briand, J.P., and Hovanessian, A.G. 1999. The anti-HIV pseudopeptide HB-19 forms a complex with the cell-surface-expressed nucleolin independent of heparan sulfate proteoglycans. J. Biol. Chem. **274**: 27875–27884.
16) Nisole, S., Krust, B., and Hovanessian, A.G. 2002 Anchorage of HIV on permissive cells leads to coaggregation of viral particles with surface nucleolin at membrane raft microdomains. Exp. Cell Res. **276**: 155–173.
17) Ratner, L., Haseltine, W., Patarca, R., Livak, K.J., Starcich, B., Josephs, S.F., Doran, E.R., Rafalski, J.A., Whitehorn, E.A., and Baumeister, K. 1985. Complete nucleotide sequence of the AIDS virus, HTLV-III. Nature **313**: 277–284.
18) Roger, B., Moisand, A., Amalric, F., and Bouvet, P. 2002. Repression of RNA polymerase I transcription by nucleolin is independent of the RNA sequence that is transcribed. J. Biol. Chem. **277**: 10209–10219.
19) Serin, G., Joseph, G., Ghisolfi, L., Bauzan, M., Erard, M., Amalric, F., and Bouvet, P. 1997. Two RNA-binding domains determine the RNA-binding specificity of nucleolin. J. Biol. Chem. **272**: 13109–13116.
20) Srivastava, M., Fleming, P.J., Pollard, H.B., and Burns, A.L. 1989. Cloning and sequencing of the human nucleolin cDNA. FEBS Lett. **250**: 99–105.
21) Srivastava, M., and Pollard, H.B. 1999. Molecular dissection of nucleolin's role in growth and cell proliferation: new insights. FASEB J. **13**: 1911–1922.
22) Takahashi, H., Matsuda, M., Kojima, A., Sata, T., Andoh, T., Kurata, T., Nagashima, K., and Hall, W.W. 1995. Human immunodeficiency virus type 1 reverse transcriptase: enhancement of activity by interaction with cellular topoisomerase I. Proc. Natl. Acad. Sci. U.S.A. **92**: 5694–5698.
23) Tokunaga, K., Greenberg, M.L., Morse, M.A., Cumming, R.I., Lyerly, H.K., and Cullen, B.R. 2002. Molecular basis for cell tropism of CXCR4-dependent human immunodeficiency virus type 1 isolates. J. Virol. **75**: 6776–6785.
24) VerPlank, L., Bouamr, F., LaGrassa, T.J., Agresta, B., Kikonyogo, A., Leis, J., and Carter, C.A. 2001. Tsg101, a homologue of ubiquitin-conjugating (E2) enzymes, binds the L domain in HIV type 1 Pr55(Gag). Proc. Natl. Acad. Sci. U.S.A. **98**: 7724–7729.
25) Zhou, W., Parent, L.J., Wills, J.W., and Resh, M.D. 1994. Identification of a membrane-binding domain within the amino-terminal region of human immunodeficiency virus type 1 Gag protein which interacts with acidic phospholipids. J. Virol. **68**: 2556–2569.
26) Zimmerman, C., Klein, K.C., Kiser, P.K., Singh, A.R., Firestein, B.L., Riba, S.C., and Lingappa, J.R. 2002. Identification of a host protein essential for assembly of immature HIV-1 capsids. Nature **415**: 88–92.

THE JOURNAL OF BIOLOGICAL CHEMISTRY
Vol. 279, No. 26, Issue of June 25, pp. 27735–27742, 2004
Printed in U.S.A.


# Nuclear Entry Mechanism of the Human Polyomavirus JC Virus-like Particle

## ROLE OF IMPORTINS AND THE NUCLEAR PORE COMPLEX*

Received for publication, October 1, 2003, and in revised form, April 6, 2004
Published, JBC Papers in Press, April 6, 2004, DOI 10.1074/jbc.M310827200

**Qiumin Qu‡, Hirofumi Sawa‡§¶, Tadaki Suzuki‡, Shingo Semba‡, Chizuka Henmi‡, Yuki Okada‡, Masumi Tsuda‡, Shinya Tanaka‡, Walter J. Atwood‖, and Kazuo Nagashima‡**

*From the ‡Laboratory of Molecular and Cellular Pathology and §21st Century COE Program for Zoonosis Control, Hokkaido University School of Medicine, and CREST, JST, Sapporo 060-8638, Japan and the ‖Department of Molecular Microbiology and Immunology, Brown University, Providence, Rhode Island 02912*

**JC virus (JCV) belongs to the polyomavirus family of double-stranded DNA viruses and causes progressive multifocal leukoencephalopathy in humans. Although transport of virions to the nucleus is an important step in JCV infection, the mechanism of this process has remained unclear. The outer shell of the JCV virion comprises the major capsid protein VP1, which possesses a putative nuclear localization signal (NLS), and virus-like particles (VLPs) consisting of recombinant VP1 exhibit a virion-like structure and physiological functions (cellular attachment and intracytoplasmic trafficking) similar to those of JCV virions. We have now investigated the mechanism of nuclear transport of JCV with the use of VLPs. Wild-type VLPs (wtVLPs) entered the nucleus of most HeLa or SVG cells. The virion structure of VLPs was preserved during transport to the nucleus as revealed by confocal microscopy of cells inoculated with fluorescein isothiocyanate-labeled wtVLPs containing packaged Cy3. The nuclear transport of wtVLPs in digitonin-permeabilized cells was dependent on the addition of importins $\alpha$ and $\beta$ and was prevented by wheat germ agglutinin or by antibodies to the nuclear pore complex. The nuclear entry of VLPs composed of VP1 with a mutated NLS was greatly inhibited, compared with that of wtVLPs, in both intact and permeabilized cells. Unlike wtVLPs, the mutant VLPs did not bind to importins $\alpha$ or $\beta$. Limited proteolysis analysis revealed that the NLS of VP1 was exposed on the surface of wtVLPs. These results suggest that JCV VLPs bind to cellular importins via the NLS of VP1 and are transported into the nucleus through the nuclear pore complex.**

Progressive multifocal leukoencephalopathy is a fatal demyelinating disease of the central nervous system and is caused by JC virus (JCV)[1] (1). Although previously rare, this condition is now commonly seen in patients of different age groups as a result of the increasingly widespread use of immunosuppressive chemotherapy and the prevalence of acquired immune deficiency syndrome (2).

JCV belongs to the polyomavirus family, which also includes simian virus 40 (SV40), murine polyomavirus, and BK virus, and is a nonenveloped, icosahedral DNA virus. The circular double-stranded DNA genome comprises 5130 bp and can be functionally divided into three regions: an early coding region, a late coding region, and a noncoding regulatory region (3). The regulatory region, which contains the promoter-enhancer for early and late gene transcription as well as the origin of DNA replication, is located between the early and late coding regions. The early gene encodes the viral regulatory protein, T antigen, whereas the late genes encode the structural capsid proteins VP1, VP2, and VP3 as well as agnoprotein.

The early events of JCV infection include attachment of the virion to the host cell surface via a receptor that contains sialic acid (4, 5). The cytoplasmic transport of JCV in eukaryotic cells is dependent on a complex network of three types of cytoskeletal elements: microtubules, microfilaments, and intermediate filaments (6). After reaching the nucleus, the viral DNA undergoes replication and is transcribed into RNA, which is followed by the production of viral proteins and virion maturation. Successful JCV infection thus depends on the import of the virion into the nucleus, but the mechanism of this import has remained unknown.

Entry of macromolecules into the nucleus is an active process and is controlled by the interactions of transport factors (importins) both with their respective macromolecular cargoes and with the nuclear pore complex (NPC) (7). The nuclear entry of proteins that contain a classical nuclear localization signal (NLS) is mediated by importin $\alpha$ and $\beta$ heterodimers (8). Importin $\alpha$ recognizes and binds directly to the NLS, whereas importin $\beta$, which interacts directly with a protein component of the nuclear pore (nucleoporin), binds the trimeric complex of the NPC and mediates its translocation into the nucleus (9).

The major capsid proteins (VP1) of SV40 and murine polyomavirus contain an NLS (10, 11). SV40 virions enter the nucleus through the NPC in a manner that is sensitive to wheat germ agglutinin (WGA) or to a monoclonal antibody specific for nucleoporin (12, 13). However, mutant SV40 virions that are devoid of an NLS have not been generated, leaving unresolved the question of whether such mutant virions would be able to enter the nucleus.

* This work was supported in part by grants from the Ministry of Education, Science, Sports, and Culture of Japan and the Ministry of Health, Labor, and Welfare, Japan. The costs of publication of this article were defrayed in part by the payment of page charges. This article must therefore be hereby marked "*advertisement*" in accordance with 18 U.S.C. Section 1734 solely to indicate this fact.

¶ To whom correspondence should be addressed: Laboratory of Molecular and Cellular Pathology, Hokkaido University School of Medicine, N15, W7, Kita-ku, Sapporo 060-8638, Japan. Tel.: 81-11-706-5053; Fax: 81-11-706-7806; E-mail: h-sawa@patho2.med.hokudai.ac.jp.

[1] The abbreviations used are: JCV, JC virus; SV40, simian virus 40; NPC, nuclear pore complex; NLS, nuclear localization signal; WGA, wheat germ agglutinin; VLP, virus-like particle; wt, wild-type; DMEM, Dulbecco's minimum essential medium; FITC, fluorescein isothiocyanate; PBS, phosphate-buffered saline; GST, glutathione *S*-transferase; TBS, Tris-buffered saline.

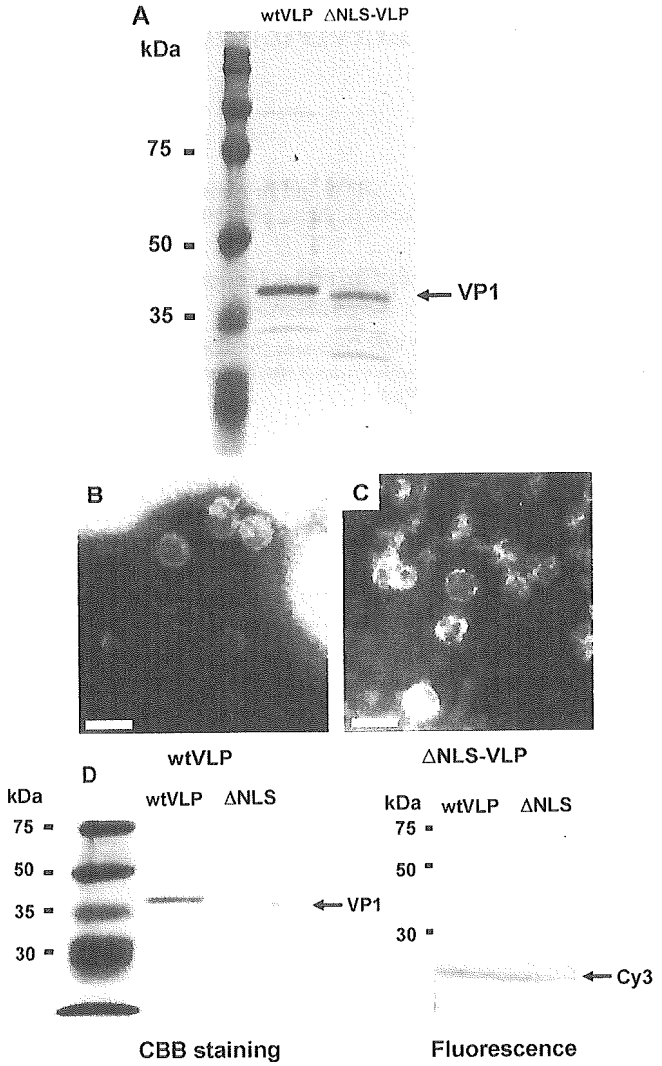


FIG. 1. **SDS-PAGE and electron microscopic analyses of VLPs composed of wtVP1 or ΔNLS-VP1.** *A*, purified wtVLPs or ΔNLS-VLPs were subjected to SDS-PAGE and Coomassie Brilliant Blue staining. The positions of the wtVP1 and ΔNLS-VP1 proteins (~45 kDa) are indicated (*arrow*). *B* and *C*, electron micrographs of wtVLPs and ΔNLS-VLPs, respectively. *Scale bars*, 60 nm. *D*, SDS-PAGE analysis of wtVLPs and ΔNLS-VLPs containing packaged Cy3. The VLPs were subjected to SDS-PAGE, and the resulting gel was stained with Coomassie Brilliant Blue to detect VP1 (*left panel*) and examined with a fluorescence image analyzer to detect Cy3 (*right panel*).

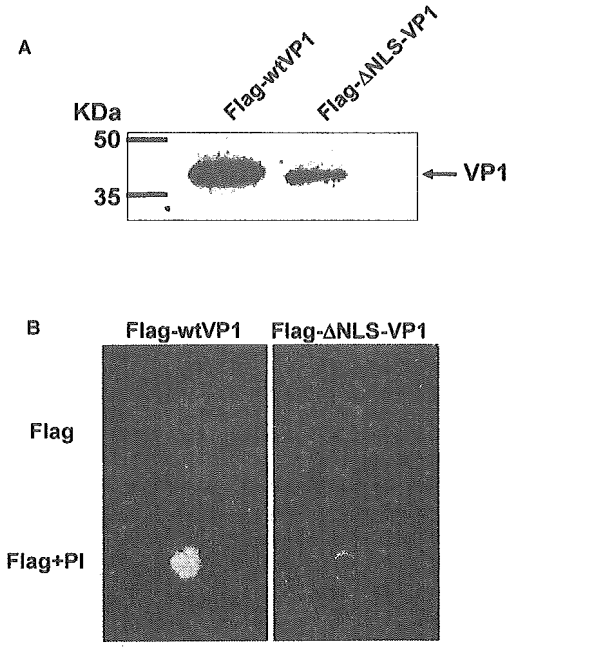


FIG. 2. **Localization of wtVP1 and ΔNLS-VP1 in transfected SVG cells.** Twenty-four hours after transfection with expression vectors encoding either FLAG-wtVP1 or FLAG-ΔNLS-VP1, the cells were harvested with RIPA buffer and subjected to immunoblot analysis (*A*) or immunofluorescence analysis (*B*) with antibodies to FLAG. The positions of the wtVP1 and ΔNLS-VP1 proteins (~45 kDa) are indicated (*arrow*). Nuclei are stained *red* with propidium iodide (*PI*) in the *lower panels* of *B*.

The $NH_2$-terminal 12 amino acids of JCV VP1 (MAPTKRKGERKD) include a stretch of basic residues that is similar to the NLS of murine polyomavirus VP1 or SV40 VP1 and is a putative NLS of JCV VP1 (14, 15). This NLS of JCV VP1 was shown to be inefficient in mediating nuclear transport (16). However, JCV virus-like particles (VLPs) consisting exclusively of recombinant VP1 purified from either *Escherichia coli* or a baculovirus-insect cell expression system and assembled by the formation of disulfide bonds (17) were found to be transported to the nucleus of host cells (18, 19). We have now investigated the mechanism of JCV nuclear entry with VLPs that exhibit both morphological characteristics and physiological functions, including hemagglutination activity, cell attachment, and cellular trafficking, similar to those of JCV virions (18–20). VLPs comprised of wild-type VP1 (wtVLPs), but not those consisting of VP1 with a mutated NLS (ΔNLS-VLPs), were imported into the nucleus of both HeLa and SVG cells. An *in vitro* transport assay revealed that wtVLPs entered the nucleus in the presence of a cytosolic fraction or of importins $\alpha$ and $\beta$, and the nuclear entry of wtVLPs was prevented by WGA or antibodies to the NPC. In addition, limited proteolysis revealed that the $NH_2$-terminal region of VP1 that includes the NLS was exposed on the outer surface of VLPs. These findings suggest that the entry of JCV VLPs into the nucleus of host cells is mediated by interaction of the NLS of VP1 with importins and the NPC.

## EXPERIMENTAL PROCEDURES

*Cell Culture*—HeLa human cervical carcinoma cells (JCRB 9004) were obtained from the Health Science Research Resources Bank (Osaka, Japan). SVG human fetal glial cells were as described (5). Both cell lines were cultured under 5% $CO_2$ at 37 °C in Dulbecco's minimum essential medium (DMEM) supplemented with 10% heat-inactivated fetal bovine serum, 2 mM L-glutamine, penicillin, and streptomycin (Sigma).

*Plasmid Construction, Cell Transfection, and Immunofluorescence Analysis*—The wtVP1 gene of JCV was subcloned from pBR-Mad1 (21) into the prokaryotic expression vector pET-15b (Novagen, Madison, WI). For construction of ΔNLS-VP1, three amino acids, $Lys^5$, $Arg^6$, and $Lys^7$, of wtVP1 were replaced with Ala, Gly, and Ala, respectively, by site-directed mutagenesis. The DNA fragment encoding ΔNLS-VP1 was also subcloned into pET-15b. To examine localization of recombinant wtVP1 and ΔNLS-VP1 in SVG cells, we subcloned the corresponding DNA fragments into the eukaryotic expression vector $pCXN_2Flag$ (22), which generates FLAG epitope-tagged recombinant proteins. The inserted DNA fragments of all plasmids were confirmed by sequencing.

Twenty-four hours after transfection of SVG cells with the use of Optifect (Invitrogen, Carlsbad, CA), cells were lysed in RIPA buffer (10 mM Tris-HCl (pH 7.5), 150 mM NaCl, 5 mM EDTA, 50 mM NaF, 10% glycerol, 1% Triton X-100, 1% sodium deoxycholate, 0.1% SDS, 0.5 mM phenylmethylsulfonyl fluoride), and expression of the recombinant proteins was confirmed by immunoblot analysis with a horseradish peroxidase-conjugated mouse monoclonal antibody to FLAG (M2, Sigma). For immunocytofluorescence analysis, the cells were fixed with 3% paraformaldehyde for 15 min at room temperature and then exposed to 70% methanol for 5 min at −20 °C. The fixed cells were incubated with the M2 antibody to FLAG (1:500 dilution), and immune complexes were detected with Alexa 488-conjugated goat antibodies to mouse immunoglobulin G (Molecular Probes, Eugene, OR). The cells were then examined with a laser-scanning confocal microscope (Olympus, Tokyo, Japan).

*Preparation of VLPs*—VLPs composed of wtVP1 or ΔNLS-VP1 were prepared as previously described (19), with slight modifications. The expression plasmids for wtVP1 and ΔNLS-VP1 were separately introduced into competent *E. coli* BL21(DE3)/pLys cells (Stratagene, La Jolla, CA) by transformation, and expression of the recombinant proteins was induced by incubation of the cells for 4 h at 30 °C with 1 mM isopropyl-β-D-thiogalactopyranoside. The cells were then separated by centrifugation for 10 min at 4,000 × *g* and resuspended in 20 ml of reassociation buffer (20 mM Tris-HCl (pH 7.5), 150 mM NaCl, 1 mM $CaCl_2$) containing lysozyme (1 mg/ml). After incubation on ice for 30 min and the addition of sodium deoxycholate to a final concentration of 2 mg/ml, the cells were incubated for an additional 10 min on ice and then lysed by five cycles of sonication (15-s bursts), and genomic DNA was digested with DNase I (Amersham Biosciences). The lysate was then centrifuged through a layer of 20% (w/v) sucrose at 100,000 × *g* for 2 h at 4 °C. The VLPs in the resulting pellet were purified further by CsCl density gradient centrifugation at 100,000 × *g* for 16 h at 16 °C. All of the gradient fractions were assayed by the hemagglutination test, and those containing the highest activity were pooled (~0.5 ml) and dialyzed for 24 h at 4 °C against two changes of reassociation buffer (1000 ml).

For conjugation with fluorescein isothiocyanate (FITC), VLPs (2 mg) were dissolved in 400 μl of phosphate-buffered saline (PBS), mixed with 40 μl of 1 M carbonate/bicarbonate buffer (pH 9.0) and 156 μl of FITC (Sigma) solution (1 mg/ml in 0.1 M carbonate/bicarbonate buffer (pH 9.0)), and incubated at room temperature for 2 h in the dark. After centrifugation of the mixture at 100,000 × *g* for 1 h at 4 °C, the pellet was dissolved in PBS and centrifuged overnight at 12,000 × *g* and 4 °C. The final pellet was resuspended in PBS. The purified VLPs composed of either wtVP1 or ΔNLS-VP1 possessed hemagglutination activity (data not shown) and yielded a prominent band of ~45 kDa on SDS-PAGE and staining with Coomassie Brilliant Blue (Fig. 1*A*). The electrophoretic mobility of ΔNLS-VP1 was slightly greater than was that of wtVP1, probably because of the difference in electrical charge between the two proteins.

*Electron Microscopic Analysis of VLPs*—VLPs (5 μl) were transferred to polyvinyl formal-coated grids and left for 5 min. After removal of residual solution with filter paper, 10 drops of 2.5% phosphotungstic acid were placed onto each grid and allowed to air dry. The VLPs were then observed with a model H-800 electron microscope (Hitachi, Tokyo, Japan). Electron microscopy revealed that both wtVLPs and ΔNLS-VLPs exhibited virion particle-like structures with a diameter of 40–50 nm (Fig. 1, *B* and *C*). A similar morphology was evident for VLPs after labeling with FITC or packaging of Cy3 (data not shown).

*Packaging of Cy3 into FITC-labeled VLPs*—The fluorescent dye Cy3 (Amersham Biosciences) contains a monofunctional NHS group for conjugation to the amino groups of proteins. To quench this reactive group, we dissolved Cy3 in 50 mM monoethanolamine and incubated the resulting solution on ice overnight. The quenched Cy3 was then packaged into FITC-labeled VLPs by the method described for the packaging of propidium iodide into JCV VLPs (23). In brief, purified FITC-labeled VLPs (0.5 mg) were dissociated in 1 ml of dissociation buffer (10 mM Tris-HCl (pH 7.5), 150 mM NaCl, 10 mM EGTA, 5 mM dithiothreitol) by incubation for 1 h at room temperature. Cy3 (100 μg) in 10 μl of 50 mM ethanolamine-HCl (pH 8.0) was added to the dissociated VP1 pentamers, and the resulting mixture was dialyzed overnight at 4 °C in the dark against 1,000 ml of reassociation buffer with a membrane that had an exclusion size of 14 kDa. After the addition of 6 mM $MgCl_2$ and 10 units of DNase I, the FITC-labeled VLPs containing Cy3 were incubated for 1 h at 37 °C, isolated by centrifugation at 100,000 × *g* for 1 h at 4 °C, and resuspended in 200 μl of PBS. To confirm that Cy3 was indeed packaged into the VLPs, we inoculated cells with a mixture of dissociated VLPs and Cy3 that had not been subjected to subsequent treatment with reassociation buffer. In addition, we subjected the FITC-labeled VLPs containing packaged Cy3 to SDS-PAGE and analyzed the resulting gel by Coomassie Brilliant Blue staining for VP1 and with a fluorescence imager (FLA 3000; Fuji Film, Tokyo, Japan) for Cy3. The fact that VP1 and Cy3 migrated at different positions in the gel confirmed that Cy3 did not bind covalently to VP1 (Fig. 1*D*).

*Packaging of DNA into VLPs and Detection of DNA by PCR*—To examine whether VLPs with packaged DNA are able to enter the nucleus, we introduced the pBluescript II SK+ plasmid (Stratagene) containing the replication origin of JCV into VLPs by the same method as that used for packaging of Cy3. HeLa or SVG cells were seeded into 60-mm plates, cultured for 24 h, and inoculated for 3 h at 37 °C either with VLPs containing DNA or with JCV in 2 ml of DMEM supplemented with 10% fetal bovine serum. Total DNA was then extracted with the use of a DNA extraction kit (Nucleobond AX; Macherey-Nagel, Easton, PA) either from total lysates of the inoculated cells or from a nuclear fraction thereof prepared as described (7).

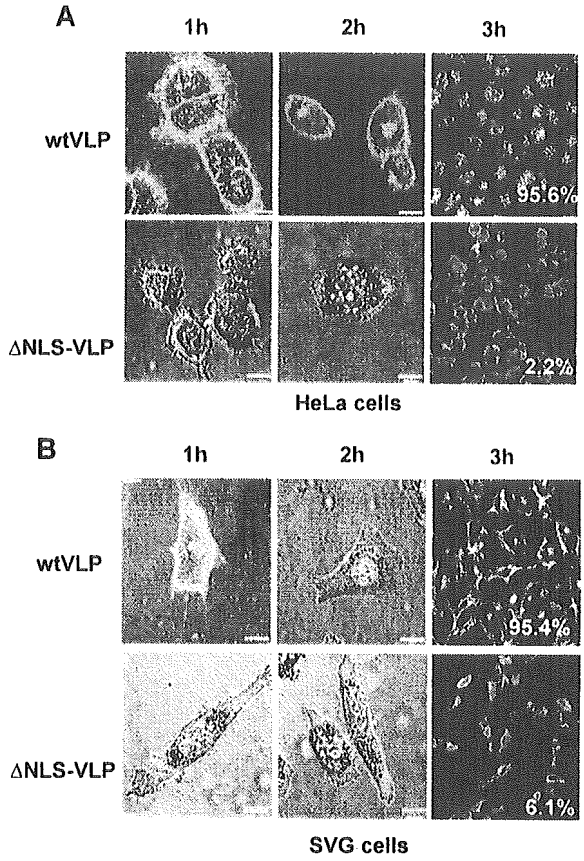


FIG. 3. **Comparison of the abilities of wtVLPs and ΔNLS-VLPs to enter the nucleus of HeLa or SVG cells.** HeLa (*A*) or SVG (*B*) cells were inoculated with FITC-labeled wtVLPs (*upper panels*) or ΔNLS-VLPs (*lower panels*). The cells were examined by confocal microscopy after 1- or 2-h subsequent incubation at 37 °C. After 3 h, the cells were fixed and then stained with propidium iodide to identify nuclei; the percentage of cells exhibiting FITC fluorescence in the nucleus was determined and is indicated in the *panels on the right*. *Scale bars*, 10 μm.

The PCR was performed with a Gene Amp PCR system 9700 (Applied Biosystems, Foster City, CA) in a 50-μl reaction mixture containing 1.0 μg of template DNA, 0.2 mM of each deoxynucleoside triphosphate, and 0.1 mM of each primer. For detection of the JCV genome, the amplification protocol included an initial incubation at 95 °C for 5 min; 30 cycles of 95 °C for 45 s, 61 °C for 30 s, and 72 °C for 30 s; and a final extension at 72 °C for 5 min. For detection of the packaged plasmid containing the JCV origin of replication, the protocol comprised an initial incubation at 95 °C for 5 min; 30 cycles of 95 °C for 30 s and 55 °C for 30 s; and a final incubation at 72 °C for 7 min. The primers for detection of the JCV genome (nucleotides 1828 to 2039) were 5′-TGTGCACTCTAATGGGCAAGC-3′ (forward) and 5′-CTAGCTACGCCTTGTGCTCTG-3′ (reverse); those for detection of the packaged plasmid were 5′-GTAAAACGACGGCCAG-3′ (forward) and 5′-CAGGAAACAGCTATGAC-3′ (reverse). The PCR products were separated by electrophoresis on an agarose gel containing ethidium bromide and visualized with ultraviolet illumination.

*Laser-scanning Confocal Microscopy*—HeLa or SVG cells (2 × $10^4$) were transferred to 35-mm glass-bottom dishes (Iwaki, Chiba, Japan) in DMEM supplemented with 10% fetal bovine serum and incubated for 24 h at 37 °C. The cells were then inoculated for 1 h at 4 °C in DMEM with FITC-labeled VLPs with or without packaged Cy3 (0.256 to 2.56 units of hemagglutination activity per cell). After three washes with PBS, the cells were incubated at 37 °C in DMEM and examined at various times with a laser-scanning confocal microscope (Olympus). For determination of the frequency of import of VLPs into the nucleus, the cells were fixed 3 h after inoculation by incubation for 10 min at room temperature with 3% paraformaldehyde and were then stained for 5 min with propidium iodide (0.2 μg/ml). The number of cells in which FITC-labeled VLPs were detected in the nucleus (as revealed by pro-

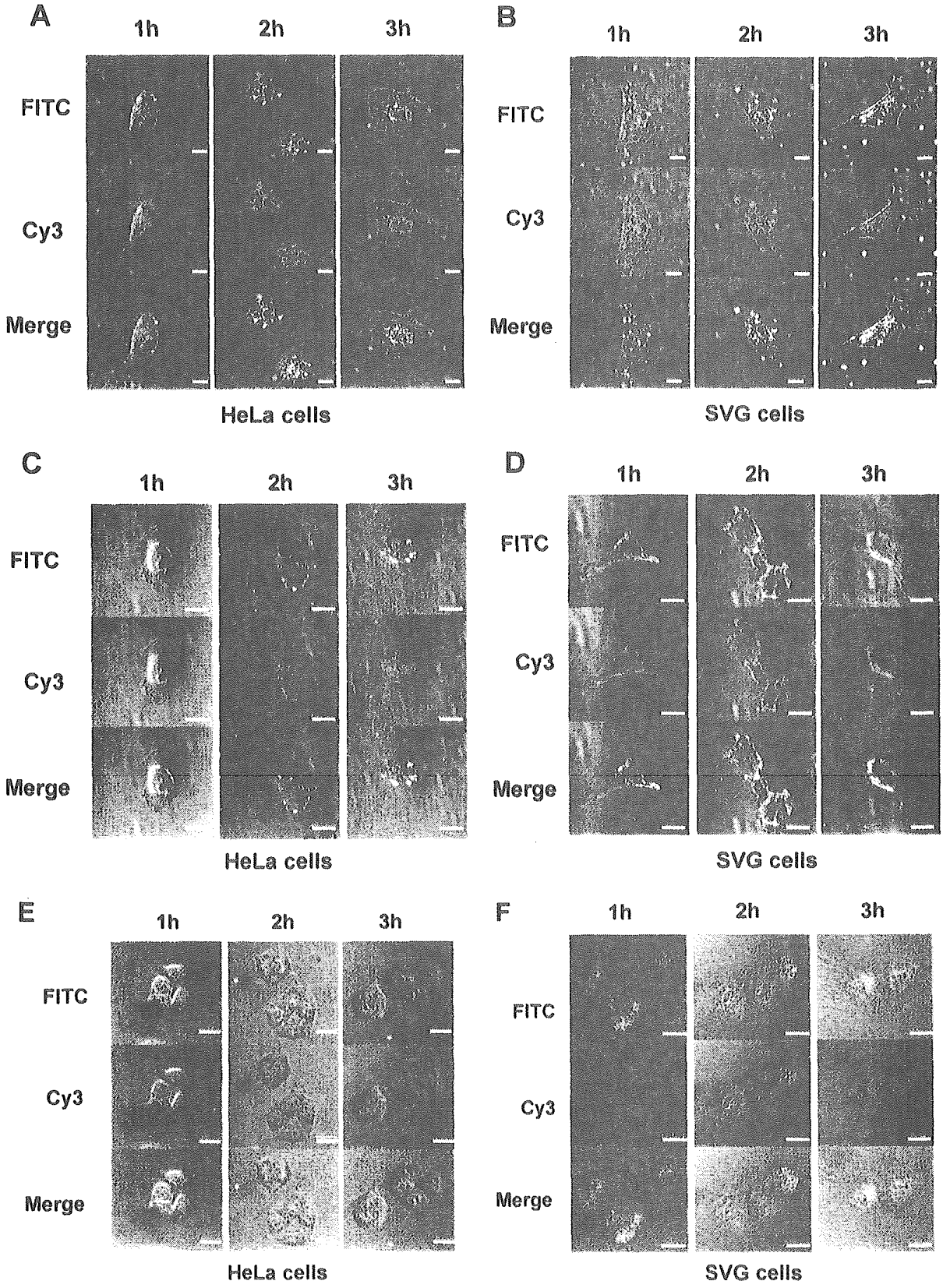


FIG. 4. **Entry of FITC-labeled wtVLPs containing packaged Cy3 into the nucleus of host cells.** *A* and *B*, HeLa or SVG cells, respectively, were inoculated with FITC-labeled wtVLPs containing packaged Cy3 and monitored for FITC (*green*) and Cy3 (*red*) fluorescence by confocal microscopy after subsequent incubation at 37 °C for the indicated times. The merged FITC and Cy3 signals are shown in *yellow*. *C* and *D*, HeLa or SVG cells, respectively, were inoculated with FITC-labeled ΔNLS-VLPs containing packaged Cy3 and monitored as in *A* and *B*. *E* and *F*, as a negative control, FITC-labeled wtVLPs were incubated in dissociation buffer for 1 h at room temperature and then mixed with Cy3 without reassociation treatment. The mixture was then used to inoculate HeLa (*E*) or SVG (*F*) cells, which were subsequently monitored for FITC and Cy3 fluorescence. *Scale bars*, 10 μm.

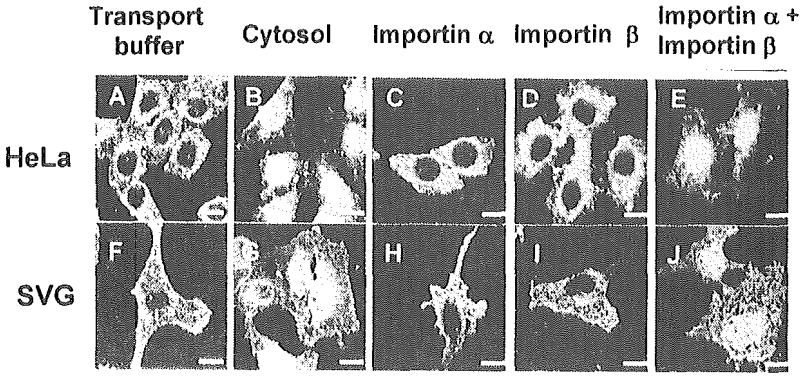


FIG. 5. **Role of importins in transport of wtVLPs into the nucleus of digitonin- permeabilized cells.** HeLa (*A–E*) or SVG (*F–J*) cells were permeabilized with digitonin and then incubated for 30 min at 37 °C with FITC-labeled wtVLPs and an ATP-regenerating system in the absence (*A* and *F*) or presence of a corresponding cytosolic fraction (*B* and *G*), GST-importin α (*C* and *H*), GST-importin β (*D* and *I*), or both GST-importins (*E* and *J*). FITC fluorescence was then examined by confocal microscopy. *Scale bars*, 10 μm.

pidium iodide staining) was counted with the laser-scanning confocal microscope and expressed as a percentage of total cells.

*In Vitro Nuclear Transport Assay*—HeLa or SVG cells were transferred to 8-well coverslips for 24 h, washed twice with a solution containing 20 mM Hepes-NaOH (pH 7.3), 110 mM potassium acetate, 5 mM sodium acetate, 2 mM magnesium acetate, and 1 mM EGTA, and then permeabilized for 5 min on ice with digitonin (90 μg/ml) in the wash solution supplemented with 2 mM dithiothreitol, 1 mM phenylmethylsulfonyl fluoride, as well as leupeptin, pepstatin, and aprotinin each at 1 μg/ml (transport buffer). This concentration of digitonin was selected as optimal from several different concentrations (40, 60, 90, and 120 μg/ml) tested. The cells were then washed three times with transport buffer and incubated first for 5 min on ice with the same solution to deplete cytosolic factors and then for 15 min at room temperature with 10 μl of transport buffer in the absence or presence of either WGA (50 μg/ml) or a mouse monoclonal antibody (200 μg/ml) to the NPC (Covance, Richmond, CA). They were washed twice with transport buffer before the addition of 10 μl of transport buffer as well as 1 μl of an ATP-regenerating system (1 mM ATP, 5 mM creatine phosphate, 20 units of creatine phosphokinase) and 10 μl of either a cytosolic fraction (68 μg of protein) or recombinant importins α or β (0.3 μg of each). After inoculation with 5 μl of FITC-labeled VLPs, the cells were incubated for 30 min at 37 °C, washed extensively with transport buffer, fixed for 10 min with 3% paraformaldehyde, and examined by laser-scanning confocal microscopy.

A cytosolic fraction was prepared as previously described (7). In brief, HeLa or SVG cells in the exponential phase of growth were harvested by centrifugation for 10 min at 900 × *g* and washed twice with ice-cold PBS. They were then washed with a solution containing 10 mM Hepes-NaOH (pH 7.3), 10 mM potassium acetate, 2 mM magnesium acetate, and 2 mM dithiothreitol, resuspended in 5 volumes of lysis buffer (5 mM Hepes-NaOH (pH 7.4), 10 mM potassium acetate, 2 mM magnesium acetate, 2 mM dithiothreitol, 20 μM cytochalasin B, 1 mM phenylmethylsulfonyl fluoride, and aprotinin, leupeptin, and pepstatin each at 1 μg/ml), incubated for 10 min on ice, and homogenized in a steel homogenizer (10 strokes). The homogenate was centrifuged at 100,000 × *g* for 40 min at 4 °C, and the resulting supernatant was dialyzed against transport buffer and then concentrated with a membrane that eliminates proteins of <10 kDa (Millipore). Recombinant importins α and β were produced in and purified from *E. coli* as glutathione *S*-transferase (GST) fusion proteins as described previously (24, 25).

*VLP Overlay Assay*—A VLP overlay assay was performed as previously described (4). Recombinant GST-importin α, GST-importin β, both importins, or GST alone were separated by SDS-PAGE on an 8% gel and then transferred to a polyvinylidene difluoride membrane. Nonspecific binding sites on the membrane were blocked by incubation for 1 h with 5% skim milk in Tris-buffered saline (TBS: 20 mM Tris-HCl (pH 7.5), 150 mM NaCl) containing 0.1% Tween 20 (TBS-T). The membrane was then incubated for 2 h at 4 °C with purified VLPs (5 μg/ml) suspended in blocking solution. After four washes with TBS-T, the membrane was incubated for 1 h at 4 °C with rabbit polyclonal antibodies (1:1000 dilution in TBS-T) to VP1 (26, 27) or GST (Amersham Biosciences). The membrane was again washed with TBS-T and then incubated for 1 h at 4 °C with horseradish peroxidase-conjugated goat $F(ab')_2$ (1:3000 dilution) to rabbit immunoglobulin (BioSource Int., Camarillo, CA). Immune complexes were detected with ECL reagents (Amersham Biosciences) and a LAS-1000 Plus image analyzer (Fuji Film).

*Limited Proteolysis of VLPs and VP1*—VLPs and VP1 were further purified by gel filtration on a column of HiLoad 16/60 Superdex 200 (Amersham Biosciences). VLPs were applied to the column after its

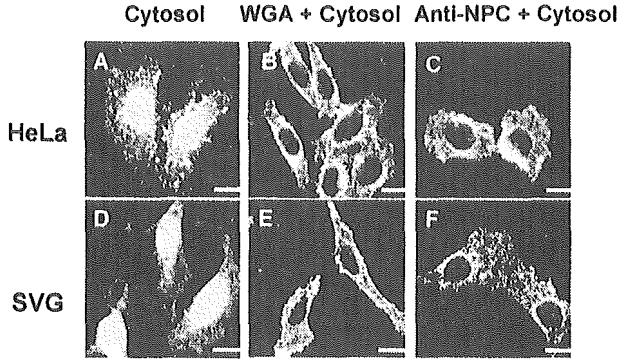


FIG. 6. **Role of the NPC in the nuclear import of wtVLPs in digitonin-permeabilized cells.** Permeabilized HeLa (*A–C*) or SVG (*D–F*) cells were pretreated in the absence (*A* and *D*) or presence of WGA (*B* and *E*) or antibodies to the NPC (*C* and *F*) and then incubated for 30 min at 37 °C with FITC-labeled wtVLPs in the presence of an ATP-regenerating system and a cytosolic fraction. *Scale bars*, 10 μm.

equilibration with TBS and eluted in the void volume with the same solution at a flow rate of 0.5 ml/min. For purification of VP1, VLPs were dialyzed against dissociation buffer overnight at 4 °C and then applied to the same column after its equilibration with dissociation buffer. VP1 monomers eluted in fractions corresponding to a molecular size of ~70 kDa. The purified VLPs and VP1 monomers were dialyzed against TBS and dissociation buffer, respectively.

For limited proteolysis, VLPs or VP1 monomers (1 mg/ml) were digested at room temperature with trypsin (10 μg/ml) (sequencing grade; Roche Diagnostics) in TBS or dissociation buffer, respectively. The reaction was terminated after various times by the addition of phenylmethylsulfonyl fluoride at a final concentration of 2 mM. The digestion products were fractionated by SDS-PAGE on a 15% gel, transferred to an Immobilon-P membrane (Millipore), and stained with Coomassie Brilliant Blue, and selected bands were excised, destained with methanol, and subjected to amino acid sequence analysis with a Procise49X cLC Protein Sequencer (Applied Biosystems).

## RESULTS

*Entry of VLPs into the Nucleus*—The function of the amino acid stretch at the $NH_2$ terminus of JCV VP1 was examined by transfecting SVG cells with expression vectors for either FLAG-wtVP1 or FLAG-ΔNLS-VP1. The electrophoretic mobility of FLAG-ΔNLS-VP1 was little greater than that of FLAG-wtVP1, which was similar to the band previously shown in Fig. 1*A*, and the expression level of FLAG-wtVP1 was slightly higher than that of FLAG-ΔNLS-VP1 (Fig. 2*A*). FLAG-wtVP1 was localized predominantly in the nucleus of SVG cells, however, FLAG-ΔNLS-VP1 was mostly restricted to the cytoplasm (Fig. 2*B*), suggesting that the basic amino acid region at the $NH_2$ terminus of VP1 functions as an NLS.

Nuclear entry of JCV VLPs was assayed by inoculating HeLa or SVG cells, which are nonpermissive and permissive, respectively, for JCV infection, with FITC-labeled VLPs. The FITC signal of wtVLPs was detected in the nucleus of HeLa cells after subsequent incubation of the cells for 1 h at 37 °C (Fig.

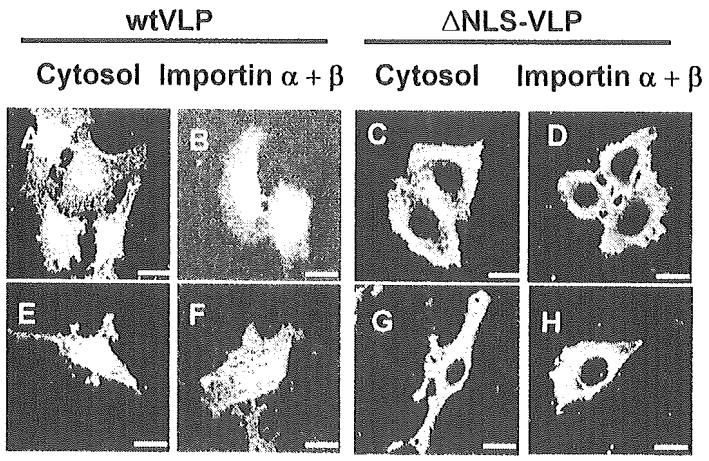


FIG. 7. **Role of the NLS of VP1 in the nuclear import of wtVLPs in digitonin-permeabilized cells.** Permeabilized HeLa (*A–D*) or SVG (*E–H*) cells were incubated for 30 min at 37 °C with FITC-labeled wtVLPs (*A*, *B*, *E*, and *F*) or ΔNLS-VLPs (*C*, *D*, *G*, and *H*) in the presence of an ATP-regenerating system and either a cytosolic fraction (*A*, *C*, *E*, and *G*) or both GST-importin α and GST-importin β (*B*, *D*, *F*, and *H*). *Scale bars*, 10 μm.

3*A*). Nuclear fluorescence increased in intensity during incubation for an additional 2 h, with 95.6% of HeLa cells containing wtVLPs in the nucleus 3 h post-inoculation. In contrast, the nuclear entry of ΔNLS-VLPs was markedly inhibited in HeLa cells, even though these particles were able to enter the cytoplasm (Fig. 3*A*). Only 2.2% of HeLa cells contained ΔNLS-VLPs in the nucleus 3 h post-inoculation. Similar results were obtained with SVG cells (Fig. 3*B*). Whereas 95.4% of SVG cells manifested wtVLPs in the nucleus 3 h post-inoculation, the corresponding value for ΔNLS-VLPs was only 6.1%. These results indicated that the NLS of VP1 is important for the nuclear translocation of VLPs in host cells.

To exclude the possibility that our detection of the FITC signal of wtVLPs in the nucleus of inoculated host cells actually represented the nuclear translocation of FITC-labeled VP1 monomers contaminating the VLP preparation, we inoculated cells with FITC-labeled wtVLPs containing packaged Cy3. The FITC (*green*) and Cy3 (*red*) signals exhibited similar temporal and spatial patterns of accumulation in the nucleus of either HeLa (Fig. 4*A*) or SVG (Fig. 4*B*) cells, indicating that FITC and Cy3 entered the nucleus as surface and internal components, respectively, of intact wtVLPs. Consistent with the results obtained with FITC-labeled ΔNLS-VLPs (Fig. 3), the FITC and Cy3 signals derived from FITC-labeled ΔNLS-VLPs containing packaged Cy3 overlapped in the cytoplasm of HeLa (Fig. 4*C*) or SVG (Fig. 4*D*) cells but did not enter the nucleus to a marked extent.

We also inoculated cells with a mixture of dissociated FITC-labeled VP1 and Cy3 that had not been subjected to reassociation treatment. The Cy3 signal was not detected within either HeLa (Fig. 4*E*) or SVG (Fig. 4*F*) cells under these conditions, indicating that Cy3 did not bind to the dissociated VP1.

*Role of Importins in the Nuclear Entry of VLPs Through the NPC*—It has been generally accepted that the NLS motif binds to importin α, which also interacts with importin β, and the resulting tripartite complex is translocated into nuclei through the NPC (28). We next examined the role of importins and the NPC in the entry of VLPs into the nucleus with digitonin-permeabilized HeLa and SVG cells. In the presence of an ATP-regenerating system, FITC-labeled wtVLPs were not able to enter the nucleus of either HeLa or SVG cells without the addition of a cytosolic fraction prepared from the corresponding intact cells (Fig. 5, *A*, *B*, *F*, and *G*), suggesting that cytosolic factors play an important role in the nuclear entry of VLPs. To determine whether such cytosolic factors might include importins, we examined the effects of GST fusion proteins of importin α or β in this system. Whereas neither importin α or β alone did not induce the nuclear translocation of wtVLPs (Fig. 5, *C*, *D*, *H*, and *I*), the combination of the two proteins did (Fig. 5, *E* and *J*).

We next tested the effect of WGA, which binds to the NPC and inhibits the import of proteins into the nucleus of intact cells (29). The nuclear import of wtVLPs apparent in digitonin-permeabilized HeLa or SVG cells in the presence of a cytosolic fraction was prevented by WGA (Fig. 6, *A*, *B*, *D*, and *E*). Furthermore, the translocation of wtVLPs into the nucleus was also completely blocked by antibodies to the NPC (Fig. 6, *C* and *F*). Together, these results thus suggested that wtVLPs entered the nucleus of host cells through the NPC. The role of the NLS of VP1 in this process was confirmed by the observation that ΔNLS-VLPs did not enter the nucleus of permeabilized HeLa or SVG cells even in the presence of a cytosolic fraction or both importin α and importin β (Fig. 7).

We investigated the possible binding of wtVLPs or ΔNLS-VLPs to importins with the use of a VLP overlay assay (4). Both GST-importin α and GST-importin β interacted with wtVLPs but not with ΔNLS-VLPs; no interaction was apparent between GST and VLPs (Fig. 8). Together, these results indicate that the nuclear import of wtVLPs is mediated by interaction of the NLS motif of VP1 with both importins α and β.

*Nuclear Entry of VLPs Containing Packaged DNA*—We also investigated whether VLPs containing packaged DNA, specifically a plasmid containing the JCV origin of replication, were able to enter the nucleus of HeLa or SVG cells. JCV DNA was detected in both total lysates and the nuclear fraction of HeLa or SVG cells after incubation of the cells for 3 h with wtVLPs containing the plasmid; the viral DNA was not detected in cell lysates after incubation of cells with a mixture of wtVLPs and nonpackaged plasmid (Fig. 9*A*). Although JCV DNA was detected in cell lysates after inoculation of cells with ΔNLS-VLPs containing the packaged plasmid, it was not detected in the nuclear fraction. As a control, we showed that JCV DNA was present in both the total lysates and nuclear fraction of cells after infection with JCV (Fig. 9*B*). Together, these results suggest that VLPs with packaged DNA are able to enter the nucleus of host cells.

*Limited Proteolysis of VLPs and VP1*—With the use of limited proteolysis, we next investigated whether the NLS motif of VP1 is exposed on the surface of wtVLPs. Incubation of VP1 monomer (purified by gel filtration) with trypsin, which cleaves proteins on the COOH-terminal side of Arg or Lys residues, resulted in the generation of a fragment of ~30 kDa (Fig. 10*A*). Digestion of purified wtVLPs with trypsin yielded several polypeptides, including an ~30-kDa fragment that appeared similar to that generated from purified VP1 as well as a 40-kDa fragment (Fig. 10*A*).

Finally, we subjected the ~30-kDa tryptic fragments of VP1 and wtVLPs to amino acid sequencing. This analysis revealed that trypsin cleaved the VP1 monomer between $Arg^{6}$ and $Lys^{7}$, whereas it cleaved wtVLPs between $Arg^{10}$ and $Lys^{11}$ of VP1 (Fig. 10*B*). Both of these cleavage sites are located within the

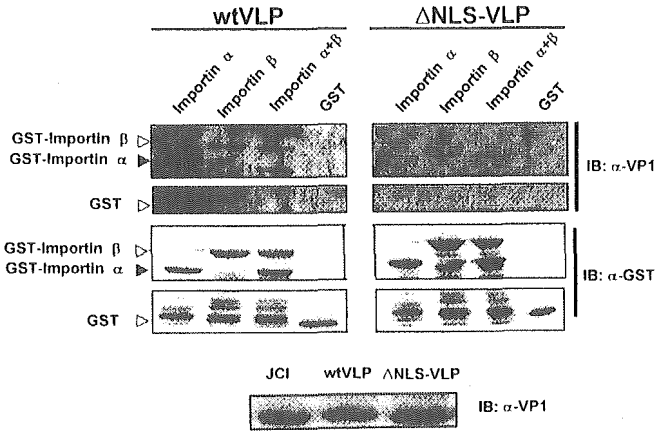


FIG. 8. **Interaction of wtVLPs with importins $\alpha$ and $\beta$ *in vitro*.** Recombinant GST-importin $\alpha$, GST-importin $\beta$, both GST-importin $\alpha$ and GST-importin $\beta$, or GST alone were subjected to SDS-PAGE and transferred to a polyvinylidene difluoride membrane. The membrane was incubated with either wtVLPs or ΔNLS-VLPs and then subjected to immunoblot analysis (*IB*) with antibodies to VP1 ($\alpha$-VP1) or GST. *Open arrowheads* indicate signals corresponding to GST-importin $\beta$ or GST; *closed arrowheads* indicate GST-importin $\alpha$. The reactivity of the antibodies to VP1 was confirmed by immunoblot analysis of a lysate of JCV-producing cells (*JCI*) as well as of purified wtVLPs and ΔNLS-VLPs (*bottom panel*).

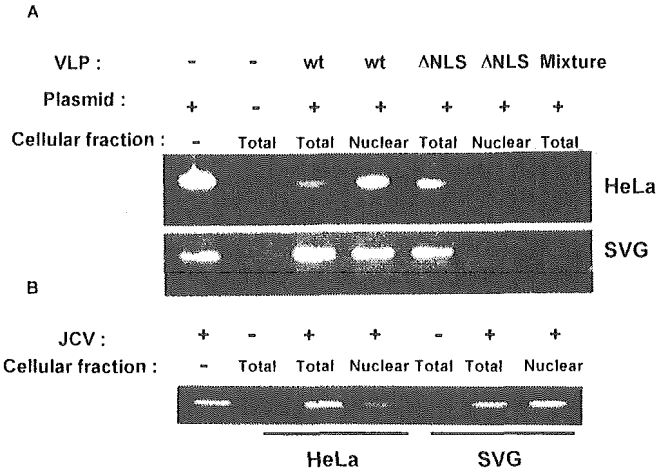


FIG. 9. **Entry of wtVLPs containing packaged DNA into the nucleus of host cells.** HeLa or SVG cells were inoculated with either wtVLPs or ΔNLS-VLPs containing a packaged plasmid that includes the JCV origin of replication (*A*) or were infected with JCV (*B*). Total cell lysates or the nuclear fractions thereof were then subjected to PCR to detect JCV DNA. As a control in *A*, cells were inoculated with a mixture of wtVLPs and plasmid without packaging treatment.

NLS, indicating that the NLS of VP1 is exposed on the surface of wtVLPs.

## DISCUSSION

In the present experiments, inoculation of cells that are permissive (SVG) or nonpermissive (HeLa) for JCV infection with wtVLPs revealed that the VLPs entered the nucleus of both cell types. We had previously shown that wtVLPs are transported to the nucleus of various other cell types (19). These observations indicate that wtVLPs are able to enter the nucleus of both permissive and nonpermissive cells, and, together with the results of previous studies (4, 19), they suggest that the neurotropism of JCV is attributable to intranuclear mechanisms such as DNA replication, transcription, or virus assembly.

Inoculation of HeLa or SVG cells with FITC-labeled wtVLPs containing packaged Cy3 resulted in the appearance of both FITC and Cy3 fluorescence signals in nuclei, whereas Cy3

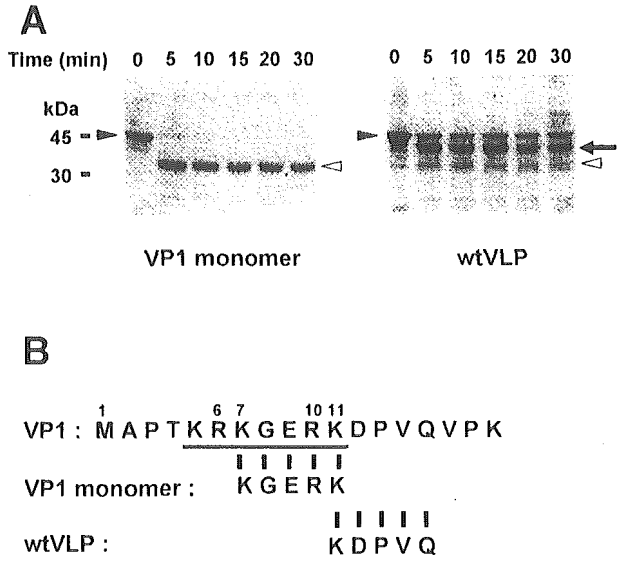


FIG. 10. **Limited proteolysis of the VP1 monomer and wtVLPs.** *A*, both the VP1 monomer and wtVLPs that had been purified by gel filtration were subjected to limited digestion with trypsin for the indicated times, after which the protein fragments were fractionated by SDS-PAGE and visualized by Coomassie Brilliant Blue staining. *Closed arrowheads* indicate full-length VP1, *open arrowheads* indicate ~30-kDa fragments, and the *arrow* indicates an ~40-kDa fragment. *B*, the $NH_2$-terminal amino acid sequences of the ~30-kDa tryptic fragments of both the VP1 monomer and wtVLPs were determined and are shown compared with the sequence of the first 18 residues of JCV VP1. The NLS motif is *underlined*.

fluorescence was not detected in cells inoculated with a mixture of dissociated FITC-labeled wtVLPs and Cy3. These results suggested that the virion structure of wtVLPs was preserved during their transport to the nucleus.

The nuclear import of wtVLPs in digitonin-permeabilized cells supplemented with an ATP-regenerating system and a cytosolic fraction was completely inhibited by WGA or by antibodies to the NPC, indicating that wtVLPs of JCV entered the nucleus through the NPC, as do SV40 virions (12). Digitonin permeabilizes the plasma membrane but leaves the nuclear envelope intact. Cells permeabilized with digitonin thus retain import-competent nuclei but are largely depleted of cytosolic components. The transport of wtVLPs to the nucleus of digitonin-permeabilized HeLa or SVG cells in the presence of an ATP-regenerating system was restored not only by a cytosolic fraction but also by recombinant importins $\alpha$ and $\beta$. We also demonstrated the ability of wtVLPs to bind to both importin $\alpha$ and $\beta$ with an overlay assay, suggesting that both importins are required for the nuclear import of wtVLPs, as has previously been shown to be the case for SV40 VP3 (30).

Proteins containing a classical NLS are transported into the nucleus after the formation of a complex with importins $\alpha$ and $\beta$. The nuclear entry of ΔNLS-VLPs was greatly inhibited in both intact and permeabilized cells. Unlike wtVLPs, ΔNLS-VLPs did not bind to importins $\alpha$ or $\beta$, suggesting that nuclear import of VLPs is mediated by interaction between importins and the NLS. The outer shell of the SV40 virion is thought to consist of 72 pentamers of VP1, with the $NH_2$-terminal region of VP1 extending across the inside of the pentamer beneath the clockwise neighboring subunit (31). In the intact SV40 virion, the NLS of VP1 is bound to the viral minichromosome and is not exposed on the virion surface (31). Rather, interaction of the NLS of VP3 in the virion with importins mediates the nuclear entry of SV40 in infected cells.

The JCV virion also comprises 72 pentamers of VP1, but its crystal structure has not been determined. With the use of limited tryptic digestion, we have now shown that the NLS

motif at the $NH_2$ terminus of JCV VP1 appears to be exposed on the surface of VLPs consisting exclusively of this protein. We were not able to synthesize JCV VLPs that include VP2 and VP3 in addition to VP1. Given the important role of the NLS of SV40 VP3 in the nuclear translocation of SV40 (30), however, it is possible that the NLS of JCV VP3 might also contribute to the entry of JCV into the nucleus.

In summary, we have shown that the nuclear translocation of JCV VLPs is dependent on the interaction between the NLS motif of VP1 and cellular importins and occurs through the NPC. These findings may serve as a basis for the development of new therapeutic strategies to combat JCV infection.

*Acknowledgments*—We thank M. Satoh and M. Sasada for technical assistance and valuable suggestions as well as Y. Abe (Center for Instrumental Analysis, Hokkaido University) for amino acid sequencing.

REFERENCES

1. Padgett, B. L., Walker, D. L., ZuRhein, G. M., Eckroade, R. J., and Dessel, B. H. (1971) *Lancet* **1,** 1257–1260
2. Dworkin, M. S. (2002) *Curr. Clin. Top. Infect. Dis.* **22,** 181–195
3. Frisque, R. J., Bream, G. L., and Cannella, M. T. (1984) *J. Virol.* **51,** 458–469
4. Komagome, R., Sawa, H., Suzuki, T., Suzuki, Y., Tanaka, S., Atwood, W. J., and Nagashima, K. (2002) *J. Virol.* **76,** 12992–13000
5. Liu, C. K., Wei, G., and Atwood, W. J. (1998) *J. Virol.* **72,** 4643–4649
6. Ashok, A., and Atwood, W. J. (2003) *J. Virol.* **77,** 1347–1356
7. Adam, S. A., Marr, R. S., and Gerace, L. (1990) *J. Cell Biol.* **111,** 807–816
8. Chi, N. C., Adam, E. J., Visser, G. D., and Adam, S. A. (1996) *J. Cell Biol.* **135,** 559–569
9. Zhang, C., Hutchins, J. R., Muhlhausser, P., Kutay, U., and Clarke, P. R. (2002) *Curr. Biol.* **12,** 498–502
10. Ishii, N., Nakanishi, A., Yamada, M., Macalalad, M. H., and Kasamatsu, H. (1994) *J. Virol.* **68,** 8209–8216
11. Chang, D., Haynes, J. I., II, Brady, J. N., and Consigli, R. A. (1992) *Virology* **191,** 978–983
12. Clever, J., Yamada, M., and Kasamatsu, H. (1991) *Proc. Natl. Acad. Sci. U. S. A.* **88,** 7333–7337
13. Yamada, M., and Kasamatsu, H. (1993) *J. Virol.* **67,** 119–130
14. Chang, D., Haynes, J. I., II, Brady, J. N., and Consigli, R. A. (1992) *Virology* **189,** 821–827
15. Ishii, N., Minami, N., Chen, E. Y., Medina, A. L., Chico, M. M., and Kasamatsu, H. (1996) *J. Virol.* **70,** 1317–1322
16. Shishido-Hara, Y., Hara, Y., Larson, T., Yasui, K., Nagashima, K., and Stoner, G. L. (2000) *J. Virol.* **74,** 1840–1853
17. Chen, P. L., Wang, M., Ou, W. C., Lii, C. K., Chen, L. S., and Chang, D. (2001) *FEBS Lett.* **500,** 109–113
18. Goldmann, C., Petry, H., Frye, S., Ast, O., Ebitsch, S., Jentsch, K. D., Kaup, F. J., Weber, F., Trebst, C., Nisslein, T., Hunsmann, G., Weber, T., and Luke, W. (1999) *J. Virol.* **73,** 4465–4469
19. Suzuki, S., Sawa, H., Komagome, R., Orba, Y., Yamada, M., Okada, Y., Ishida, Y., Nishihara, H., Tanaka, S., and Nagashima, K. (2001) *Virology* **286,** 100–112
20. Chang, D., Fung, C. Y., Ou, W. C., Chao, P. C., Li, S. Y., Wang, M., Huang, Y. L., Tzeng, T. Y., and Tsai, R. T. (1997) *J. Gen. Virol.* **78,** 1435–1439
21. Okada, Y., Sawa, H., Tanaka, S., Takada, A., Suzuki, S., Hasegawa, H., Umemura, T., Fujisawa, J., Tanaka, Y., Hall, W. W., and Nagashima, K. (2000) *J. Biol. Chem.* **275,** 17016–17023
22. Tokui, M., Takei, I., Tashiro, F., Shimada, A., Kasuga, A., Ishii, M., Ishii, T., Takatsu, K., Saruta, T., and Miyazaki, J. (1997) *Biochem. Biophys. Res. Commun.* **233,** 527–531
23. Goldmann, C., Stolte, N., Nisslein, T., Hunsmann, G., Luke, W., and Petry, H. (2000) *J. Virol. Methods* **90,** 85–90
24. Imamoto, N., Shimamoto, T., Kose, S., Takao, T., Tachibana, T., Matsubae, M., Sekimoto, T., Shimonishi, Y., and Yoneda, Y. (1995) *FEBS Lett.* **368,** 415–419
25. Imamoto, N., Shimamoto, T., Takao, T., Tachibana, T., Kose, S., Matsubae, M., Sekimoto, T., Shimonishi, Y., and Yoneda, Y. (1995) *EMBO J.* **14,** 3617–3626
26. Okada, Y., Sawa, H., Endo, S., Orba, Y., Umemura, T., Nishihara, H., Stan, A. C., Tanaka, S., Takahashi, H., and Nagashima, K. (2002) *Acta Neuropathol. (Berl.)* **104,** 130–136
27. Okada, Y., Endo, S., Takahashi, H., Sawa, H., Umemura, T., and Nagashima, K. (2001) *J. Neurovirol.* **7,** 302–306
28. Gorlich, D., Pante, N., Kutay, U., Aebi, U., and Bischoff, F. R. (1996) *EMBO J.* **15,** 5584–5594
29. Dabauvalle, M. C., Schulz, B., Scheer, U., and Peters, R. (1988) *Exp. Cell Res.* **174,** 291–296
30. Nakanishi, A., Shum, D., Morioka, H., Otsuka, E., and Kasamatsu, H. (2002) *J. Virol.* **76,** 9368–9377
31. Liddington, R. C., Yan, Y., Moulai, J., Sahli, R., Benjamin, T. L., and Harrison, S. C. (1991) *Nature* **354,** 278–284

Journal of Medical Virology 74:668–676 (2004)

# Investigation of Simian Virus 40 Large T Antigen in 18 Autopsied Malignant Mesothelioma Patients in Japan

**Mulan Jin,[1,3] Hirofumi Sawa,[1,2,3]* Tadaki Suzuki,[1,3] Kazuko Shimizu,[1] Yoshinori Makino,[1,3] Shinya Tanaka,[1,3] Takayuki Nojima,[4] Yasunori Fujioka,[5] Makoto Asamoto,[6] Noriaki Suko,[7] Miri Fujita,[8] and Kazuo Nagashima[1,3]**

[1]*Laboratory of Molecular & Cellular Pathology, Hokkaido University School of Medicine, Sapporo, Japan*
[2]*21st Century COE Program for Zoonosis Control, Hokkaido University School of Medicine, Sapporo, Japan*
[3]*CREST, JST, Sapporo, Japan*
[4]*Department of Clinical Pathology, Kanazawa Medical University, Ishikawa, Japan*
[5]*Department of Pathology, Kyorin University School of Medicine, Tokyo, Japan*
[6]*First Department of Pathology, Nagoya City University Medical School, Nagoya City, Japan*
[7]*Department of Internal Medicine, Iwamizawa Municipal Hospital, Iwamizawa, Japan*
[8]*Department of Pathology, Shinnittetsu Muroran General Hospital, Muroran, Japan*

It has been reported that Simian virus 40 (SV40) is linked to human beings by inoculation of contaminated poliovaccines and may have a role in the etiology of malignant mesothelioma. However, there have been no reports describing the relationship between SV40 and malignant mesothelioma in Japan. A study was undertaken to investigate whether SV40 was related to patients of malignant mesothelioma in Japan by the polymerase chain reaction (PCR) assay, DNA sequence analysis, and immunohistochemical methods. Paraffin-embedded samples of the 18 autopsied patients with pleural malignant mesothelioma were collected from five hospitals in Japan. After isolation of DNA from paraffin blocks, PCR analyses followed by sequencing were performed using three different sets of primers for detection of SV40 large T antigen (TAg) gene. All 18 malignant mesothelioma samples were also immunohistochemically evaluated for expression of SV40 TAg protein with two different anti-SV40 TAg antibodies. SV40 TAg genome was detected in eight malignant mesothelioma cases. Only one of three primer pairs successfully amplified SV40 genome in the samples, whereas all pairs yielded a PCR product in the controls, suggesting a low content of virus DNA. No immunopositive staining for SV40 TAg was found in any of the samples. This study shows that SV40 genome was present in a subset of Japanese malignant mesothelioma patients who were unlikely to have received a contaminated polio vaccine based on their age. ***J. Med. Virol. 74:668–676, 2004.*** © 2004 Wiley-Liss, Inc.



**KEY WORDS:** SV40; malignant mesothelioma; PCR; sequence; immunohistochemistry

## INTRODUCTION

In the past 50 years, the incidence of malignant mesothelioma has been increasing gradually along with industrial development [Carbone et al., 2002; Ishikawa et al., 2003]. It has been well documented that malignant mesothelioma is a neoplasm associated with asbestos exposure [Carbone et al., 2002]; however, no definite evidence of exposure to asbestos could be found in the work histories of some patients [Pairon et al., 1994; Hirvonen et al., 1999]. These investigations suggest that there are other factors involved in the pathogenesis of malignant mesothelioma.

Simian virus 40 (SV40), which belongs to the polyomavirus family, is a DNA virus that can cause variable types of animal tumors, such as osteosarcoma, brain tumor, and lymphoma [Diamandopoulos, 1973; Carbone

Grant sponsor: Ministry of Education, Science, Technology, Sports, and Culture of Japan, the Ministry of Health, Labor, and Welfare of Japan, and the Japan Human Science Foundation.

*Correspondence to: Hirofumi Sawa, MD, PhD, Laboratory of Molecular & Cellular Pathology, Hokkaido University School of Medicine, N-15, W-7, Kita-ku, Sapporo 060-8638, Japan.
E-mail: h-sawa@patho2.med.hokudai.ac.jp

Accepted 17 August 2004
DOI 10.1002/jmv.20219
Published online in Wiley InterScience (www.interscience.wiley.com)

et al., 1998]. The oncogenic potential of SV40 is mainly regulated by the early protein, large T antigen (TAg) that is expressed in the nuclei of virus-infected cells and can promote cellular transformation through the interaction with tumor suppressor genes, including p53 and those of the retinoblastoma (Rb) gene family [De Luca et al., 1997; Carbone et al., 1997a].

SV40 has been reported to transfer to humans by contaminated poliovirus vaccines that had been used widely in Western countries before 1963 [Carbone et al., 2002]. As for the relationship between SV40 and malignant mesothelioma, SV40 was first reported to be linked to malignant mesothelioma in 1993 by Cicala and coworkers who induced successfully malignant mesothelioma within 6 months in 30 of 34 hamsters by direct injection of the virus into the chest cavity of animals [Cicala et al., 1993]. In addition, the virus genome has been demonstrated in malignant mesothelioma and other human neoplasms, such as non-Hodgkin's lymphoma, brain tumor, and osteosarcoma [Bergsagel et al., 1992; Carbone et al., 1994; Rizzo et al., 1998; Shivapurkar et al., 2002], However, relevant research has not been reported in Japanese malignant mesothelioma cases. Hence, the purpose of this study was to investigate whether SV40 is related to Japanese malignant mesothelioma. In order to detect SV40, polymerase chain reaction (PCR) for SV40 TAg genome was undertaken following DNA sequence analysis and immunohistochemical staining for SV40 Tag, which is known as a viral oncogenic protein.

## MATERIALS AND METHODS

### Tumor Samples

Eighteen autopsy samples of Japanese patients with pleural malignant mesothelioma were collected from five hospitals in Japan. The formalin-fixed and paraffin-embedded tissues were stained with hematoxylin and eosin (H&E) and examined immunohistochemically for expression of calretinin (anti-calretinin polyclonal antibody, Zymed Laboratories, South San Francisco, CA), a specific marker of malignant mesothelioma [Ordonez,

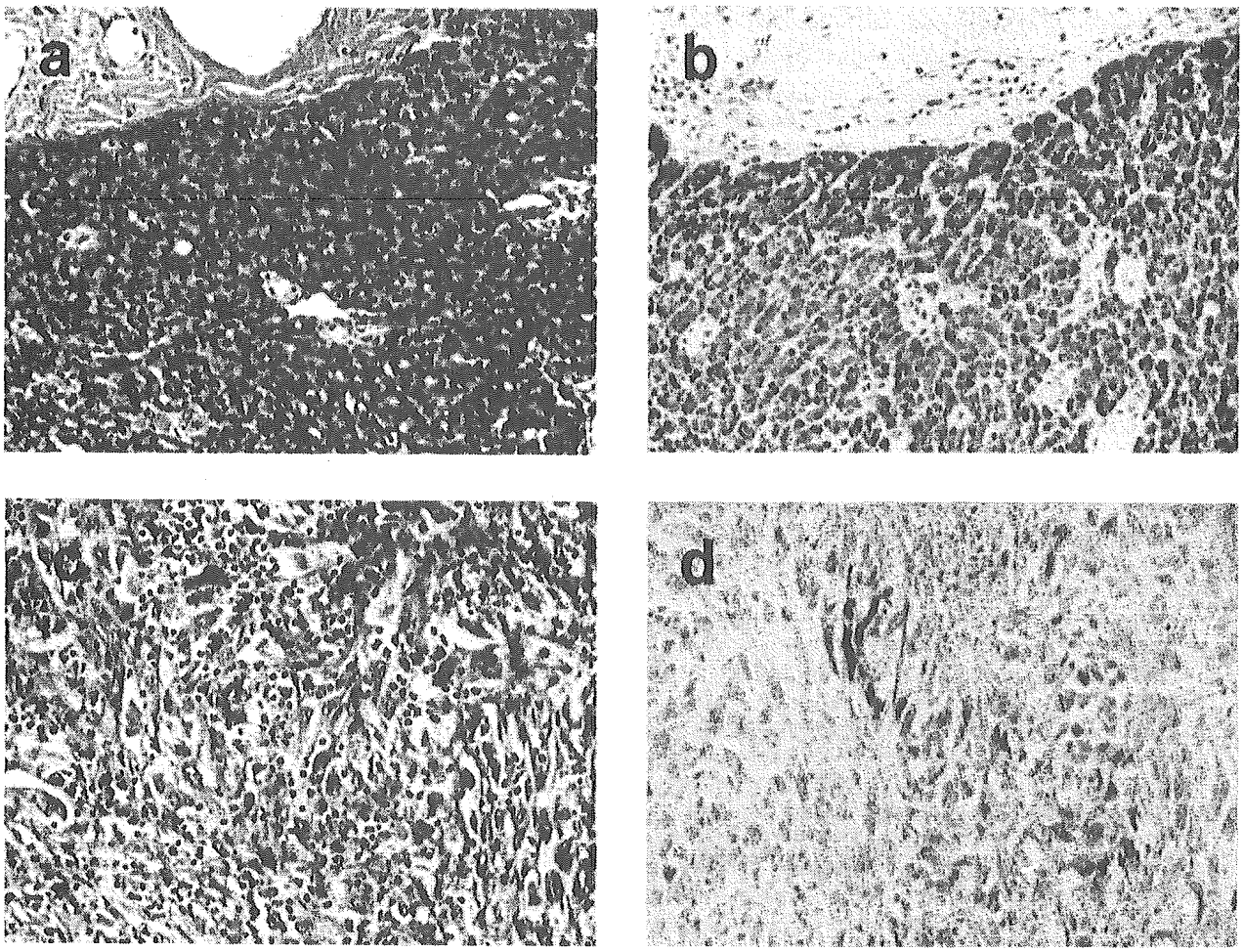


Fig. 1. Hematoxylin & eosin (H&E) and immunohistochemical staining of representative malignant mesothelioma cases. **a**: The epithelioid mesothelioma grows as solid sheets of cuboidal cells with oval nuclei and eosinophilic cytoplasm (40×). **b**: Almost all the cells of the epithelioid mesothelioma have immunopositive signals against calretinin (40×). **c**: The biphasic mesothelioma contains more sarcomatoid components than epitheliod mesothelioma (40×). **d**: Calretinin is dominantly expressed in epitheliod tumor cells (40×).

2003] (Fig. 1). Two pathologists examined independently these H&E sections. There were 13 male and 5 female patients with an age range from 36 to 83 years (mean; 61.9), which included a case of asbestos associated desmoplastic malignant mesothelioma [Ishikawa et al., 2003]. Two 7-μm sections of each sample were prepared to extract DNA for PCR, and another 2-μm section adjacent to those 7-μm ones was stained with H&E to confirm the presence of tumors in the sections for DNA extraction. Furthermore, two 2-μm sections were examined with immunohistochemical staining using anti-SV40 TAg antibodies. Each block was separately cut with a new microtome knife to avoid contamination of samples examined.

### Cells and Tissue Samples as Control Experiments

HEK293T cell line expressing SV40 TAg was used as a positive control for the PCR to detect SV40 genome and immunohistochemistry. In addition, prostate tumor tissue samples from the SV40 TAg-transgenic rat [Asamoto et al., 2001] were used as a positive control for the immunohistochemical study. HEK293 (JCRB 9068) and HEK293JCT cell lines that express TAg of JC virus (JCV), which belongs to polyomavirus similarly as SV40, were used as negative controls. HEK293 cells were purchased from the Health Science Research Resources Bank (HSRRB, Osaka, Japan). All cell lines were maintained in Dulbecco's minimal essential medium supplemented with 10% fetal bovine serum and antibiotics (penicillin and streptomycin) from Sigma (St. Louis, MO). These cells were treated with trypsin and centrifuged at 1,500 rpm at 4°C for 5 min to harvest. The pellet was washed with phosphate buffered saline (PBS) and fixed by neutralized formalin overnight. After fixation,cells were embedded into paraffin and applied to PCR and immunohistochemical analyses.

### Extraction of DNA From Paraffin-Embedded Tissues

Two 7-μm sections from each sample were prepared separately with a disposable microtome knife to avoid contamination of examined samples, and deparaffinized with xylene. Thereafter, the tissue was washed with 99.5% of ethanol twice, and resuspended with 180 μl of the lysis solution (GenElute Mammalian Genomic DNA Kit, Sigma) and 20 μl of 10 mg/ml proteinase K solution. The sample was incubated overnight at 55°C until tissue became completely dissolved. Proteinase K was then inactivated by heating at 70°C for 10 min. Cellular debris was removed by centrifuging at 12,000 rpm for 5 min. DNA was extracted with the GenElute Mammalian Genomic DNA Kit according to the manufacturers' protocol.

### PCR Detection of SV40 Genome

In order to verify the quality of DNA from paraffinmbedded tissue, a 157-bp fragment of human K-*ras* gene, which belongs to a Ras multigene family in the human, was amplified initially using primer sets A (+) and B (−) (5′-ACT GAA TAT AAA CTT GTG GTA GTT GGA CCT-3′ and 5′-TCA AAG AAT GGT CCT GGA CC-3′) [Levi et al., 1991]. Only a specimen sample that could amplify the K-*ras* fragment was selected for subsequent study. In this experiment, three different sets of primers were used for detection of the SV40 gene, including SV.for3: 5′-TGA GGC TAC TGC TGA CTC TCA ACA-3′ from nucleotides 4476 to 4453, and SV.rev: 5′-GCA TGA CTC AAA AAA CTT AGC AAT TCTG-3′ from nucleotides 4399 to 4372 [Lednicky and Butel, 1998]; PYV.for: 5′-TAG GTG CCA ACC TAT GGA ACAGA-3′ from nucleotides 4574 to 4552, and PYV.rev: 5′-GGA AAG TCT TTA GGG TCT TCTAACC-3′ from nucleotides 4425 to 4402 [Bergsagel et al., 1992]; and TA1: 5′-GAC CTG TGG CTG AGT TTG CTC A-3′ from nucleotides 3070 to 3049, and TA2: 5′-GCT TTA TTT GTA ACC ATT ATA AG-3′ from nucleotide 2652 to 2630 [Lednicky and Butel, 1998] that amplified a 105-bp fragment of the SV40-specific TAg gene [Lednicky and Butel, 1998], a 172-bp fragment of the N-terminus of SV40 TAg gene [Bergsagel et al., 1992], and a 441-bp fragment of the C-terminus of SV40 TAg gene, respectively [Lednicky and Butel, 1998]. The PCR conditions of these primers are described in Table I, and the position of the primer sets are represented in Figure 2. As a negative control for PCR, DNA was also extracted from autopsied liver samples of four patients with positive PCR reaction for SV40 TAg in malignant mesothelioma samples. The PCR reaction was performed using an Ampil Tag Gold (PE Biosystems, Foster City, CA).

### DNA Cloning and Sequencing

The PCR products using primers SV.for3 and SV.rev, were subcloned into a pGEM-T Easy vector (Promega, Madison, WI). Sequencing-grade plasmid DNA was purified with a GenElute Plasmid Miniprep Kit (Sigma),

TABLE I. Parameters of the PCR Reactions

| | SV.for3/SV.rev | | PYV.for/PYV.rev | | TA1/TA2 | |
|---|---|---|---|---|---|---|
| | Temperature | Time | Temperature | Time | Temperature | Time |
| Denaturation | 95°C | 10 min | 94°C | 3 min | 95°C | 7 min |
| Number of cycles | 50 | | 50 | | 55 | |
| Denaturation | 94°C | 30 sec | 94°C | 60 sec | 95°C | 30 sec |
| Annealing | 60°C | 30 sec | 52°C | 60 sec | 53°C | 30 sec |
| Extension | 72°C | 60 sec | 72°C | 60 sec | 72°C | 30 sec |

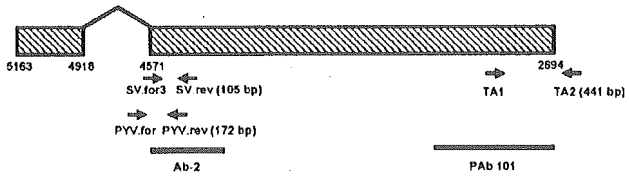


Fig. 2. The position of the used PCR primers and the epitopes of antibodies which were used in this study. The hatched boxes represent the exon regions of the SV40 TAg genome. The small numbers under the boxes correspond with the nucleotide positions according to the numbering system used for SV40 of Buchman et al. [1981]. The arrows indicate the orientation of the primers from 5′ to 3′. The underlines indicate the epitope region of the antibodies.

and sequenced in both the sense and antisense directions by a sequensor (ABI, Foster City, CA). Sequence data were analyzed by alignment with SV40 complete genome sequence (NCBI-AY271817).

### Immunohistochemical Staining

All the samples were examined immunohistochemically with two different mouse anti-SV40 TAg monoclonal antibodies: PAb 101 (PharMingen, San Diego, CA) and Ab-2 (Oncogene Science, Boston, MA). The epitopes of these antibodies are shown in Figure 2. The specificity of these antibodies was confirmed by immunoblotting using cell lines of HEK293, HEK293T, and HEK293JCT. Immunoblotting was carried out as described previously [Okada et al., 2000]. Briefly, cell lysates from each cell line were resolved by an SDS–polyacrylamide gel electrophoresis (SDS–PAGE), transferred onto nitrocellulose filters, and immunoblotted with each antibody. Immunoreactive bands were detected with an anti-Ig conjugated with horseradish peroxidase followed by ECL (Amersham Pharmacia Biotech, Piscataway, NJ) and analyzed with a LAS-1000 plus (Fuji Film, Tokyo, Japan).

The tissue was processed as described previously with slight modifications [Okada et al., 2002]. Briefly, formalin-fixed, paraffin-embedded sections were deparaffinized with xylenes and rehydrated with ethanol. As a positive control for immunostaining prostate tumour tissue samples from the SV40 TAg-transgenic rats was used [Asamoto et al., 2001]. For antigen retrieval, sections were treated in a pressure cooker for 3 min in the presence of 0.01 M of citrate buffer. After washing with deionized water, sections were treated with 1% of $H_2O_2$ in methanol to quench the endogenous peroxidase activity and normal rabbit serum, and thereafter incubated with primary antibody at 4°C overnight. Specimens from tissues PAb101 were diluted at 1: 250, and Ab-2 was diluted at 1: 400. These antibodies were diluted at 1: 2,000 for specimens from cell lines. Following incubation with the biotinylated anti-mouse immunoglobulins (Nichirei, Tokyo, Japan) and the peroxidase-labeled streptavidin reagent (Nichirei), immunopositive signals were visualized using 3,3′-diaminobenzidine tetrahydrochloride (DAB) as a chromogen and counterstained with a hematoxylin.

## RESULTS

Initially, the PCR assays with three different primer sets, which had been used to detect SV40 TAg DNA [Bergsagel et al., 1992; Lednicky and Butel, 1998], were applied, using DNAs extracted from paraffin-embedded tissues. All the DNAs from the paraffin-embedded malignant mesothelioma tissues and the control cell lines yielded products of 157 bp of K-*ras* gene (Tables II and III, and Fig. 3). The results of PCR using three sets of primers for SV40 (Fig. 3 and Table I) are summarized in Tables II and III. SV40 TAg genome could be detected in paraffin-embedded 293T cells expressing SV40 TAg;

TABLE II. Results of PCR, DNA Sequence, and Immunohistochemistry

| Patient | Birth & death years | Sex | Tumor type | DNA control | SV.for3/ SV.rev | Sequencing | PYV.for/ PYV.rev | TA1/TA2 | Immuno-histochemistry |
|---|---|---|---|---|---|---|---|---|---|
| 1 | 1928 & 1995 | M | S | + | + | + | − | − | − |
| 2 | 1916 & 2001[a] | F | S | + | + | + | − | − | − |
| 3 | 1935 & 1998 | F | E+S | + | − | ND | − | − | − |
| 4 | 1944 & 1996 | M | E+S | + | + | + | − | − | − |
| 5 | 1940 & 1994 | M | E+S | + | − | ND | − | − | − |
| 6 | 1945 & 2002 | M | E | + | − | ND | − | − | − |
| 7 | 1930 & 2003 | M | E | + | + | + | − | − | − |
| 8 | 1949 & 2001 | M | S | + | − | ND | − | − | − |
| 9 | 1950[b] & 2002 | M | E | + | − | ND | − | − | − |
| 10 | 1949 & 2002 | M | E | + | − | ND | − | − | − |
| 11 | 1923 & 2001 | F | E | + | + | + | − | − | − |
| 12 | 1941 & 1996 | M | S | + | + | + | − | − | − |
| 13 | 1927 & 1995 | M | S | + | + | + | − | − | − |
| 14 | 1906 & 1983 | M | E+S | + | + | + | − | − | − |
| 15 | 1953[b] & 1989 | F | E | + | − | ND | − | − | − |
| 16 | 1952[b] & 2002 | M | E | + | − | ND | − | − | − |
| 17 | 1948 & 2002 | F | E | + | − | ND | − | − | − |
| 18 | 1914 & 1995 | M | E | + | − | ND | − | − | − |

+, positive results; −, negative results; E, epithelial type; S, sarcomatous type; E + S: biphasic type; ND, not done.
[a]Asbestos associated case [Ishikawa et al., 2003].
[b]They might have been presumably inoculated because of having been born in the 1950s.

TABLE III. Controls of PCR and Immunohistochemistry Assays

| | Virus genome | DNA control (K-ras) | SV.for3/SV.rev | PYV.for/PYV.rev | TA1/TA2 | Immunohistochemistry (Pab101/Ab-2) |
|---|---|---|---|---|---|---|
| 293T | SV40 TAg | + | + | + | + | +/+ |
| 293JCT | JC virus TAg | + | − | + | − | −/+ |
| 293 | None | + | − | − | − | −/− |

however, no signal was recognized in 293JCT or 293 cells with the SV.for3/SV.rev and TA1/TA2 primer sets (Table III). As for the PYV.for/PYV.rev primers, a positive signal was obtained in DNA samples from 293JCT cells as well as 293T cells as described previously [Bergsagel et al., 1992] (Table III).

In 8 samples of 18 malignant mesothelioma samples (44.4%) including an asbestos-associated case, a 105 bp-fragment of SV40-specific TAg gene using SV.for3/SV.rev could be detected (Fig. 3), and no positive PCR reaction was recognized using both PYV.for/PYV.rev and TA1/TA2 primer sets (Table II). Sequencing analysis revealed that each 105-bp amplified DNA product with SV.for3/SV.rev primer sets was consistent with the SV40 TAg genome according to the data from GenBank (NCBI-AY271817) (Table II). The liver samples of four patients with positive PCR reaction for TAg in malignant mesothelioma samples were verified to be negative in this PCR assay (data not shown).

To investigate SV40TAg protein expression, immunohistochemical analyses were carried out using two independent anti-SV40 TAg monoclonal antibodies: pAb101 and Ab-2.

Immunoblotting revealed that PAb 101 recognized exclusively SV40 TAg. In contrast, an intense signal was detected in the lysates from 293JCT cells as well as from 293T cells using Ab-2 antibody, suggesting that Ab-2 crossreacts with JCV TAg (Fig. 4).

The immunohistochemical data are summarized in Tables II and III, and representative results are illustrated in Figure 5. The positive controls, including prostate tumor tissue from the SV40 transgenic rat (Fig. 5a) and HEK293T cell line (Fig. 5b), showed consistently strong and intense nuclear staining with PAb 101 antibody in almost all the cells, but no positive staining was demonstrated in HEK293 or HEK293JCT cells (Fig. 5c,d). Immunostaining using Ab-2 antibody demonstrated nuclear positivity in HEK293JCT cell lines (Fig. 5e) as well as in HEK293T cells (Fig. 5f) and prostate tumor cells from the SV40 transgenic rat (data not shown). Among 18 malignant mesothelioma samples, both PAb 101 and Ab-2 antibodies failed to demonstrate positive nuclear staining (Fig. 5g,h). Both antibodies for SV40 TAg did not exhibit positive staining in a negative control sample from HEK293 cell lines (Fig. 5c and data not shown). Faint dot-like signals in the nuclei were detected in a few tumor cells in three samples using PAb 101 antibody (Fig. 5g), but these signals were not considered to be significant in comparison with those of prostate tumor tissue from the

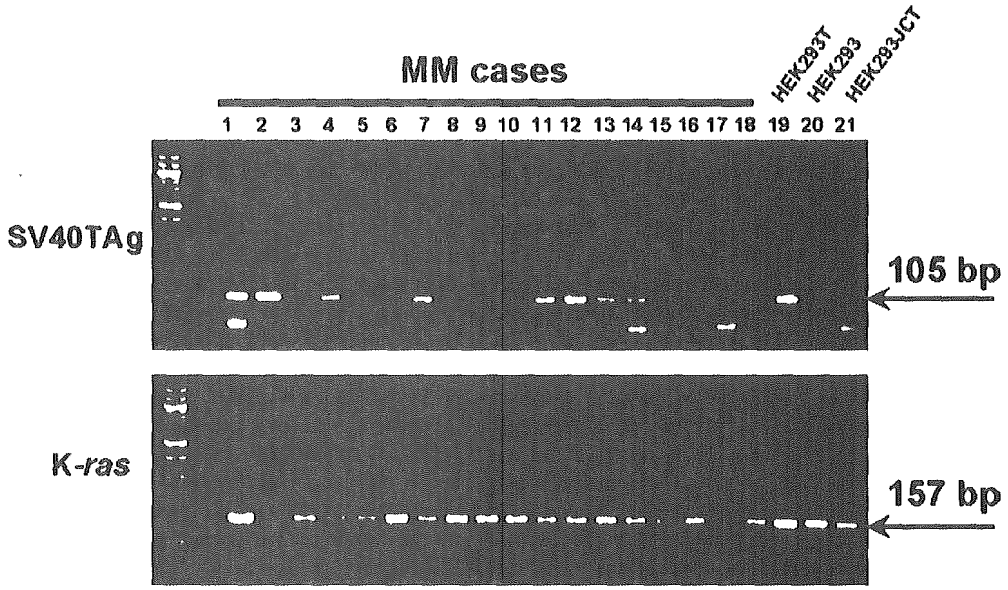


Fig. 3. PCR analysis of SV40-specific TAg gene in 18 malignant mesothelioma patients. The PCR primers (SV.for3 and SV.rev) were designed to amplify the region with the length of 105 bp (4476–4372 nt) of the SV40 TAg gene. **Lanes 1–18**, **19**, **20**, and **21** are representative samples from 18 malignant mesothelioma tissues, HEK293T cells, HEK293 cells, and HEK293JCT cells, respectively. In an agarose gel electrophoresis, lanes 1, 2, 4, 7, 11, 12, 13, and 14 demonstrated positive signals for SV40 TAg, while lanes 3, 5, 6, 8, 9, 10, 15, 16, 17, and 18 were negative. Lane 19 (HEK293T) was a positive control, and lanes 20 (HEK293) and 21 (HEK293JCT) were negative controls for the primer sets. The K-*ras* gene (157 bp) was amplified as a control reaction.

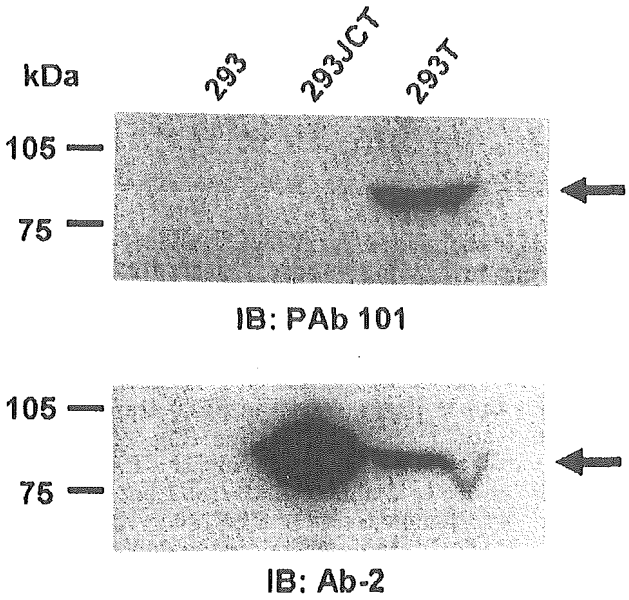


Fig. 4. Western blot analysis with two different monoclonal antibodies against SV40 TAg. The lanes are representative for cells lysated from HEK293 (293), HEK293JCTT (293JCT), and HEK293T cell lines (293T), respectively. The signal of SV40 TAg protein was exclusively detected in HEK293T cells using PAb 101 antibody (**upper panel**). The Ab-2 antibody recognized JCV TAg and SV40 TAg (**lower panel**). The arrows indicate the signals of TAg.

SV40 transgenic rat (Fig. 5a) and HEK293T cell line (Fig. 5b).

## DISCUSSION

SV40 TAg is the primary viral gene product responsible for SV40 replication and SV40 mediated cellular transformation [Ray et al., 1990]. In order to detect SV40 oncogenic TAg gene, three separate regions of the genetic TAg genome, which were usually applied to the investigation of association of the virus with cancers [Bergsagel et al., 1992; De Luca et al., 1997; Lednicky and Butel, 1998], were amplified. They contained the 105-bp region flanking the gene encoding the Rb-binding site [De Luca et al., 1997], the N-terminal 172-bp region covering the Rb-p107-Rb2/p130 binding domain [Bergsagel et al., 1992], and the C-terminal 441-bp region located in a p53 binding domain [Stewart et al., 1996; Lednicky and Butel, 1998; Arrington et al., 2000]. In several previous studies, the presence of SV40 TAg gene was determined on the simultaneously positive signals in two or three different PCR assays [Bergsagel et al., 1992; Capello et al., 2003]. Eight positive samples were obtained from 18 malignant mesothelioma, all for a 105-bp region. No positive samples were obtained for the 172- and 441-bp fragments. The discrepancy between PCR and the published results might be explained by following facts. The final result of PCR-based studies is highly dependent on the PCR conditions. Generally, primers that give smaller products may result in a higher sensitivity for viral DNA detection [Griffiths et al., 1998]. DNA damage and degradation in formalin fixation might result in a lower probability of generating longer products including the 172 and 441 bp in the present study [Arrington and Butel, 2001]. An alternative explanation might be related to the relatively small amount of paraffin-embedded tissue, and consequently the total yield of DNA might be lower [Arrington and Butel, 2001]. Because of the above problems, sequence analysis to strengthen the reliability of the results of the PCR reaction was carried out. It was confirmed that no SV40 TAg was recognized in liver samples of the patients containing SV40 TAg in malignant mesothelioma samples. This finding is therefore helpful for excluding false positive results.

The expression of TAg was not detected immunohistochemically, presumably owing to the lack expression or to the rapid degradation of TAg, either of which might be caused by long-term fixation in formalin [Simsir et al., 2001]. The same interpretation could apply to the fact that TAg was well demonstrated in the tumors of the experimental animals, which were immediately fixed by formalin after death. Alternatively, in an established or growing tumor, it is possible that SV40 might replicate without detectable expression of TAg under a specific condition, for instance, where both the p53 and pRB pathways have deteriorated [Kouhata et al., 2001], and the amount of viral DNA sequences might be much lowered, resulting in inability to TAg express [Ricciardiello et al., 2003].

The presence of SV40 in 60% of human malignant mesothelioma was shown by Carbone et al. [1994], and similar results were reported in several independent investigations [Strickler et al., 1996; Shivapurkar et al., 1999]. It has already been stated that humans are susceptible to SV40 [Butel and Lednicky, 1999; Carbone et al., 2003]. SV40 was thought to be introduced accidentally into human beings between 1955 and 1963 by SV40-contaminated poliovaccines [Shah and Nathanson, 1976; Carbone et al., 1997b]. Millions of people, including children and adults, in the United States, Canada, and Europe were inoculated during that period [Shah and Nathanson, 1976]. In Japan, the poliovaccine was carried out in 1962 and 1963 [Yamamoto et al., 2000], during which time almost all Japanese children between 3 months and 12 years of age were inoculated the oral live vaccine imported from Canada and the USSR [Yamamoto et al., 2000]. However, no SV40 genome was found in our 10 patients, although 3 (Cases 9, 15, and 16) born from 1950 to 1953 were in the inoculated population. On the other hand, the remaining 8 patients who were considered not to have been inoculated based on their age were positive for SV40 TAg. These observations implied that some of the Japanese malignant mesothelioma patient might be related to SV40 exposure without receiving vaccines. It has been verified that human infection with SV40 could occur by the other routes, for instance interhuman spread with in addition to the exposure to contaminated vaccine [Butel and Lednicky, 1999; Kwak et al., 2002; Carbone et al., 2003]. In this study, for example, there was one asbestos-associated case (Case 2).

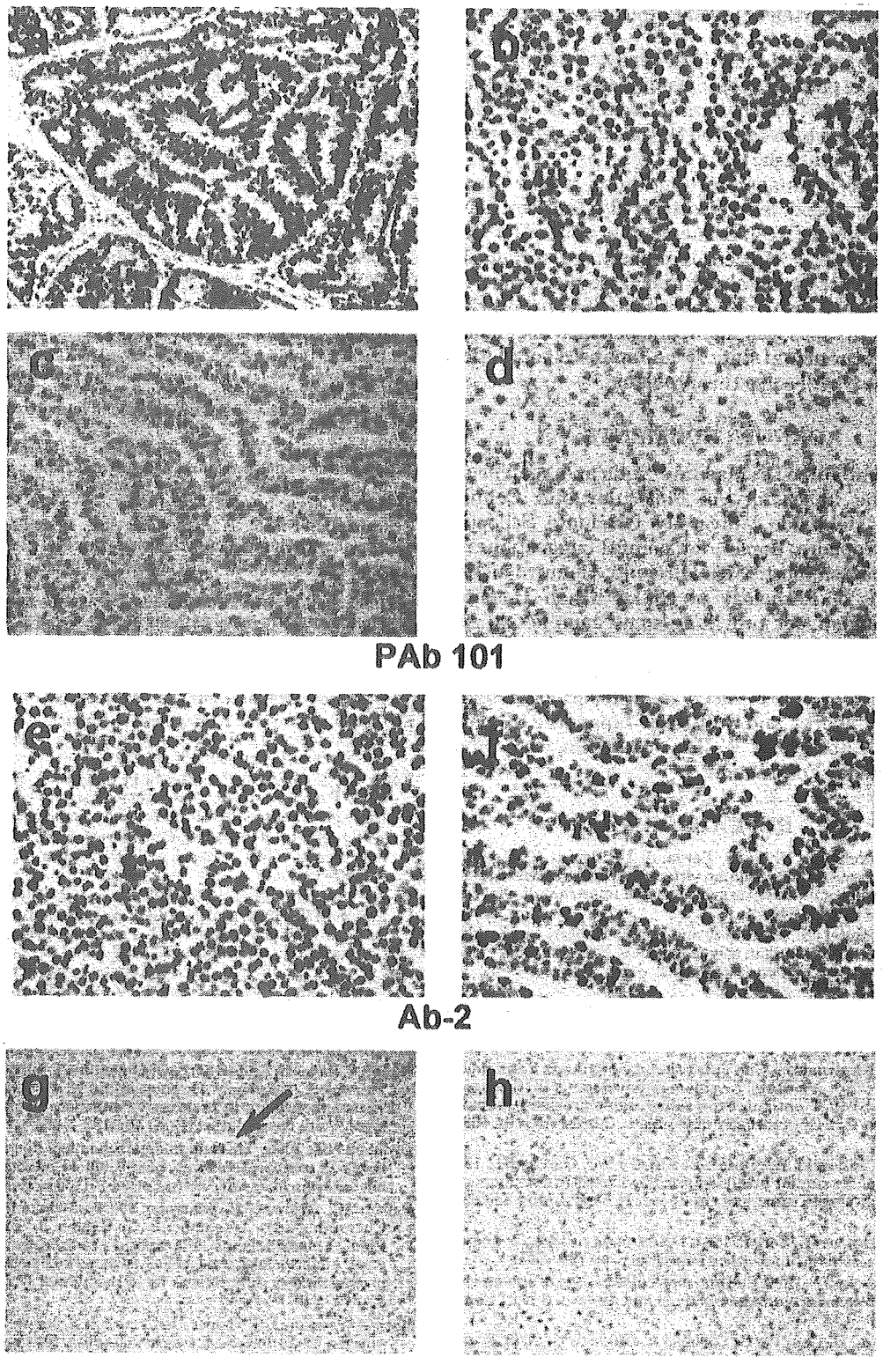


Fig. 5. The immunohistochemical analysis of TAg in SV40 TAg-transformed prostate tumor tissue, cell lines, and malignant mesothelioma samples. **a**: The prostate tumor tissue in SV40 TAg-transgenic rat showed strong nuclear staining with anti-TAg antibody (PAb 101, 400×). **b**: A similar nuclear staining was observed in the HEK293T cell block section (PAb 101, 400×). **c**, **d**: No immunoreactivity was found with anti-TAg mAb (PAb 101, 400×) in HEK293 and HEK293JCT cell block sections, respectively. **e**, **f**: HEK293JCT and HEK293T cell block sections demonstrated strong nuclear staining with anti-TAg mAb (Ab-2, 400×). **g**, **h**: No positive immunoreaction was recognized in the malignant mesothelioma samples by both PAb 101 and Ab-2 antibodies, respectively. The dot-like signal in the nucleus was found in very few cells in an malignant mesothelioma sample (black arrow, g).

It has been reported that SV40 may synergize with asbestos in the pathogenesis of malignant mesothelioma [Aldieri et al., 2004; Carbone and Rdzanek, 2004]. More cases are needed to determine the possible relationship between SV40 and asbestos.

There were a number of limitations in our study. Generally, to avoid lack of sensitivity for viral DNA detection, frozen or fresh tissues should be used for PCR analysis. However, frozen malignant mesothelioma tissue could not be obtained and false-negative PCR results may have occurred as a consequence. In addition, the number of cases was small, and perhaps not enough to represent the actual state of the Japanese population. A larger study will solve this problem.

## ACKNOWLEDGMENTS

We are grateful to Dr. Masumi Tsuda and Ms. Yasuko Orba of the Laboratory of Molecular and Cellular Pathology, Hokkaido University Graduate School of Medicine, Sapporo, Japan, for helpful suggestion and technological support; Mr. Hiroyuki Uemura of the Department of Pathology of Nikko Kinen Hospital, Muroran, Japan, for providing some samples. Mulan Jin is a Research Fellow of the Japan Society for the Promotion of Science. This work was supported in part by grants from the Ministry of Education, Science, Technology, Sports, and Culture of Japan, the Ministry of Health, Labor, and Welfare of Japan, the Japan Human Science Foundation.

## REFERENCES

Aldieri E, Orecchia S, Ghigo D, Bergandi L, Riganti C, Fubini B, Betta PG, Bosia A. 2004. Simian virus 40 infection down-regulates the expression of nitric oxide synthase in human mesothelial cells. Cancer Res 64:4082–4084.

Arrington AS, Butel JS. 2001. SV40 and human tumors. In: Khalili K, Stoner GL, editors. Human polyomaviruses: Molecular and clinical perspectives. 1st edition. New York: John Wiley & Sons, Inc. pp 461–490.

Arrington AS, Lednicky JA, Butel JS. 2000. Molecular characterization of SV40 DNA in multiple samples from a human mesothelioma. Anticancer Res 20:879–884.

Asamoto M, Hokaiwado N, Cho YM, Takahashi S, Ikeda Y, Imaida K, Shirai T. 2001. Prostate carcinomas developing in transgenic rats with SV40 T antigen expression under probasin promoter control are strictly androgen dependent. Cancer Res 61:4693–4700.

Bergsagel DJ, Finegold MJ, Butel JS, Kupsky WJ, Garcea RL. 1992. DNA sequences similar to those of simian virus 40 in ependymomas and choroid plexus tumors of childhood. N Engl J Med 326:988–993.

Buchman AR, Burnet L, Berg P. 1981. DNA tumor viruses. In: Tooze J, editor. NY: Cold Spring Harbor Laboratory. pp 799–841.

Butel JS, Lednicky JA. 1999. Cell and molecular biology of simian virus 40: Implications for human infections and disease. J Natl Cancer Inst 91:119–134.

Capello D, Rossi D, Gaudino G, Carbone A, Gaidano G. 2003. Simian virus 40 infection in lymphoproliferative disorders. Lancet 361:88–89.

Carbone M, Rdzanek MA. 2004. Pathogenesis of malignant mesothelioma. Clin Lung Cancer 5:S46–S50.

Carbone M, Pass HI, Rizzo P, Marinetti M, Di Muzio M, Mew DJ, Levine AS, Procopio A. 1994. Simian virus 40-like DNA sequences in human pleural mesothelioma. Oncogene 9:1781–1790.

Carbone M, Rizzo P, Grimley PM, Procopio A, Mew DJ, Shridhar V, de Bartolomeis A, Esposito V, Giuliano MT, Steinberg SM, Levine AS, Giordano A, Pass HI. 1997a. Simian virus-40 large-T antigen binds p53 in human mesotheliomas. Nat Med 3:908–912.

Carbone M, Rizzo P, Pass HI. 1997b. Simian virus 40, poliovaccines and human tumors: A review of recent developments. Oncogene 15: 1877–1888.

Carbone M, Stach R, Di Resta I, Pass HI, Rizzo P. 1998. Simian virus 40 oncogenesis in hamsters. Dev Biol Stand 94:273–279.

Carbone M, Kratzke RA, Testa JR. 2002. The pathogenesis of mesothelioma. Semin Oncol 29:2–17.

Carbone M, Burck C, Rdzanek M, Rudzinski J, Cutrone R, Bocchetta M. 2003. Different susceptibility of human mesothelial cells to polyomavirus infection and malignant transformation. Cancer Res 63: 6125–6129.

Cicala C, Pompetti F, Carbone M. 1993. SV40 induces mesotheliomas in hamsters. Am J Pathol 142:1524–1533.

De Luca A, Baldi A, Esposito V, Howard CM, Bagella L, Rizzo P, Caputi M, Pass HI, Giordano GG, Baldi F, Carbone M, Giordano A. 1997. The retinoblastoma gene family pRb/p105, p107, pRb2/p130 and simian virus-40 large T-antigen in human mesotheliomas. Nat Med 3:913–916.

Diamandopoulos GT. 1973. Induction of lymphocytic leukemia, lymphosarcoma, reticulum cell sarcoma, and osteogenic sarcoma in the Syrian golden hamster by oncogenic DNA simian virus 40. J Natl Cancer Inst 50:1347–1365.

Griffiths DJ, Nicholson AG, Weiss RA. 1998. Detection of SV40 sequences in human mesothelioma. Dev Biol Stand 94:127–136.

Hirvonen A, Mattson K, Karjalainen A, Ollikainen T, Tammilehto L, Hovi T, Vainio H, Pass HI, Di Resta I, Carbone M, Linnainmaa K. 1999. Simian virus 40 (SV40)-like DNA sequences not detectable in Finnish mesothelioma patients not exposed to SV40-contaminated polio vaccines. Mol Carcinog 26:93–99.

Ishikawa R, Kikuchi E, Jin M, Fujita M, Itoh T, Sawa H, Nagashima K. 2003. Desmoplastic malignant mesothelioma of the pleura: Autopsy reveals asbestos exposure. Pathol Int 53:401–406.

Kouhata T, Fukuyama K, Hagihara N, Tabuchi K. 2001. Detection of simian virus 40 DNA sequence in human primary glioblastomas multiforme. J Neurosurg 95:96–101.

Kwak EJ, Vilchez RA, Randhawa P, Shapiro R, Butel JS, Kusne S. 2002. Pathogenesis and management of polyomavirus infection in transplant recipients. Clin Infect Dis 35:1081–1087.

Lednicky JA, Butel JS. 1998. Consideration of PCR methods for the detection of SV40 in tissue and DNA specimens. Dev Biol Stand 94:155–164.

Levi S, Urbano-Ispizua A, Gill R, Thomas DM, Gilbertson J, Foster C, Marshall CJ. 1991. Multiple K-ras codon 12 mutations in cholangiocarcinomas demonstrated with a sensitive polymerase chain reaction technique. Cancer Res 51:3497–3502.

Okada Y, Sawa H, Tanaka S, Takada A, Suzuki S, Hasegawa H, Umemura T, Fujisawa J, Tanaka Y, Hall WW, Nagashima K. 2000. Transcriptional activation of JC virus by human T-lymphotropic virus type I Tax protein in human neuronal cell lines. J Biol Chem 275:17016–17023.

Okada Y, Sawa H, Endo S, Orba Y, Umemura T, Nishihara H, Stan AC, Tanaka S, Takahashi H, Nagashima K. 2002. Expression of JC virus agnoprotein in progressive multifocal leukoencephalopathy brain. Acta Neuropathol (Berl) 104:130–136.

Ordonez NG. 2003. The immunohistochemical diagnosis of mesothelioma: A comparative study of epithelioid mesothelioma and lung adenocarcinoma. Am J Surg Pathol 27:1031–1051.

Pairon JC, Orlowski E, Iwatsubo Y, Billon-Galland MA, Dufour G, Chamming's S, Archambault C, Bignon J, Brochard P. 1994. Pleural mesothelioma and exposure to asbestos: Evaluation from work histories and analysis of asbestos bodies in bronchoalveolar lavage fluid or lung tissue in 131 patients. Occup Environ Med 51:244–249.

Ray FA, Peabody DS, Cooper JL, Cram LS, Kraemer PM. 1990. SV40 T antigen alone drives karyotype instability that precedes neoplastic transformation of human diploid fibroblasts. J Cell Biochem 42:13–31.

Ricciardiello L, Baglioni M, Giovannini C, Pariali M, Cenacchi G, Ripalti A, Landini MP, Sawa H, Nagashima K, Frisque RJ, Goel A, Boland CR, Tognon M, Roda E, Bazzoli F. 2003. Induction of chromosomal instability in colonic cells by the human polyomavirus JC virus. Cancer Res 63:7256–7262.

Rizzo P, Di Resta I, Stach R, Mutti L, Picci P, Kast WM, Pass HI, Carbone M. 1998. Evidence for and implications of SV40-like

sequences in human mesotheliomas and osteosarcomas. Dev Biol Stand 94:33–40.

Shah K, Nathanson N. 1976. Human exposure to SV40: Review and comment. Am J Epidemiol 103:1–12.

Shivapurkar N, Wiethege T, Wistuba II, Salomon E, Milchgrub S, Muller KM, Churg A, Pass H, Gazdar AF. 1999. Presence of simian virus 40 sequences in malignant mesotheliomas and mesothelial cell proliferations. J Cell Biochem 76:181–188.

Shivapurkar N, Harada K, Reddy J, Scheuermann RH, Xu Y, McKenna RW, Milchgrub S, Kroft SH, Feng Z, Gazdar AF. 2002. Presence of simian virus 40 DNA sequences in human lymphomas. Lancet 359:851–852.

Simsir A, Fetsch P, Bedrossian CW, Ioffe OB, Abati A. 2001. Absence of SV-40 large T antigen (Tag) in malignant mesothelioma effusions: An immunocytochemical study. Diagn Cytopathol 25: 203–207.

Stewart AR, Lednicky JA, Benzick US, Tevethia MJ, Butel JS. 1996. Identification of a variable region at the carboxy terminus of SV40 large T-antigen. Virology 221:355–361.

Strickler HD, Goedert JJ, Fleming M, Travis WD, Williams AE, Rabkin CS, Daniel RW, Shah KV. 1996. Simian virus 40 and pleural mesothelioma in humans. Cancer Epidemiol Biomarkers Prev 5: 473–475.

Yamamoto H, Nakayama T, Murakami H, Hosaka T, Nakamata T, Tsuboyama T, Oka M, Nakamura T, Toguchida J. 2000. High incidence of SV40-like sequences detection in tumour and peripheral blood cells of Japanese osteosarcoma patients. Br J Cancer 82:1677–1681.